AMERICAN MUSEUM
Novitates

PUBLISHED BY THE AMERICAN MUSEUM OF NATURAL HISTORY
CENTRAL PARK WEST AT 79TH STREET, NEW YORK, NY 10024
Number 3371, 33 pp., 18 figures, 1 table June 21, 2002

The Osteology of *Matutinia* (Simplicidentata, Mammalia) and Its Relationship to *Rhombomylus*

SUYIN TING,[1] JIN MENG,[2] MALCOLM C. McKENNA,[3] AND CHUANKUEI LI[4]

ABSTRACT

New dental, cranial, and postcranial specimens of the eurymylid *Matutinia nitidulus* from the early Eocene Lingcha Formation, Hengyang Basin, Hunan Province, China, are described. These materials are among the best of basal gliroid mammals from Asia. *Matutinia* is similar to *Rhombomylus* in general tooth and cranial morphologies, including an expanded hypocone shelf on the upper cheek teeth and a complex zygomatic arch. These features distinguish the two genera from other eurymylids such as *Heomys* and *Eurymylus*. *Matutinia* differs from *Rhombomylus* in having lower crowned and less lophate cheek teeth, fewer bony septa in the mastoid chamber, a lower promontorium, and a carotid foramen in the ear region. Based on the new material, we consider *Matutinia* a valid genus, not a junior synonym of *Rhombomylus*.

INTRODUCTION

Matutinia nitidulus is a member of the Eurymylidae, an endemic Asian eutherian group (Matthew et al., 1929; McKenna and Bell, 1997). The family was originally based on *Eurymylus laticeps*, represented by a maxilla from the late Paleocene Gashato fauna of Mongolia, and was originally placed in ?Plesiadapidae (Matthew and Granger, 1925). In the same paper, Matthew and Granger (1925) named *Baenomys ambiguus* on the basis of

[1] LSU Museum of Natural Science, Louisiana State University, Baton Rouge, LA 70803; e-mail: glsuyin@lsu.edu; Institute of Vertebrate Paleontology and Paleoanthropology, Chinese Academy of Sciences, P.O. Box 643, Beijing 100044, P.R. China.
[2] Assistant Curator, Division of Paleontology, American Museum of Natural History; e-mail: jmeng@amnh.org
[3] Curator Emeritus, Division of Paleontology, American Museum of Natural History.
[4] Institute of Vertebrate Paleontology and Paleoanthropology, Chinese Academy of Sciences, P.O. Box 643, Beijing 100044, P. R. China.

 ISSN 0003-0082

a dentary, and they regarded the species as family indeterminate in the Glires. Following the discovery of additional specimens, Matthew et al. (1929) synonymized *Baenomys ambiguus* with *Eurymylus laticeps*. Because *Eurymylus* possesses features similar to both rodents and lagomorphs, Matthew et al. (1929) assigned the then monotypic family Eurymylidae to ?Glires. The Eurymylidae was later placed respectively in the Lagomorpha (Wood, 1942; Simpson, 1945), the monotypic order Mixodontia (Sych, 1971), or the Anagalida along with the Pseudictopidae, Zalambdalestidae, and Anagalidae (Szalay and McKenna, 1971; Ting and Li, 1984; Li and Ting, 1985). Currently, the family Eurymylidae contains about a dozen genera, which are characterized by having one pair of upper incisors, but lacking some rodent features (Dashzeveg and Russell, 1988; Li and Ting, 1985, 1993; Averianov, 1994; McKenna and Bell, 1997). Eurymylids are commonly accepted as the closest relatives of Rodentia (Li and Ting, 1985, 1993; Li et al., 1987; Averianov, 1994; Meng et al., 1994; McKenna and Bell, 1997), although they may be a paraphyletic group (Averianov, 1994; Meng et al., 1994; Meng and Wyss, 1994, 2001).

Li et al. (1979) named and briefly described *Matutinia nitidulus* based on jaw specimens collected from the early Eocene Lingcha Formation, Hengyang Basin, Hunan Province, China. No detailed description, comparison, or discussion of this taxon has since been published. Li et al. (1979: 77) briefly diagnosed the specimens as ''a form intermediate between *Heomys* and *Rhombomylus*, premolar non-molarized, metaconule rudimentary, posterior margin of the palate ends at the line of the middle of M2, paraconid reduced. The enamel of cheek teeth massive''. In reviewing the Paleocene and Eocene ''Mixodontia'' of Mongolia and China, Dashzeveg and Russell (1988: 149) argued that the p4 of *M. nitidulus* shows ''approximately intermediate characters'' between *Rhombomylus turpanensis* and *Rhombomylus laianensis*; that ''no diagnostic distinguishing features of generic value are evident from the lower teeth''; and that ''a difference in shape of M3 appears to be the major distinction separating this species from *R. turpanensis*; difference in crown height seems negligible''. Thus, Dashzeveg and Russell (1988: 150) were ''unable to justify the generic distinction of *Matutinia* from *Rhombomylus*'' and considered *M. nitidulus* as a species of *Rhombomylus*, with which *Matutinia* became a junior synonym. McKenna and Bell (1997) followed this synonymy.

Previously undescribed, relatively complete fossils of *M. nitidulus*, including dental, cranial, and postcranial elements, were collected from the type locality. With few exceptions, other eurymylids are represented only by fragmentary jaws and teeth. The new specimens of *Matutinia* therefore provide significant new information on the morphology, phylogeny, and evolution of early glidroid mammals. The purpose of this study is to describe the new specimens, and, by comparing *Matutinia* with *Rhombomylus* and other eurymylids, to determine the taxonomic status of *Matutinia*. The broader phylogenetic implications of these new materials will be discussed elsewhere.

MATERIALS AND METHODS

All specimens described here are housed in the Institute of Vertebrate Paleontology and Paleoanthropology (IVPP), Chinese Academy of Sciences, and were collected from the early Eocene Lingcha Formation in Hengyang Basin, Hunan Province, China (fig. 1). The description and comparison of the teeth and cranium of *Matutinia nitidulus* are mainly based on IVPP V7443-5. The morphology of the postcranial skeleton is based solely on IVPP V7444. All photographs were taken with a RT SPOT digital camera and edited using Adobe Photoshop. Photographs of dentitions are taken on casts (figs. 2, 3). Cranial terminology follows Novacek (1986). Terminology for the postcrania follows Miller (1964), Romer (1966), and Szalay (1985). Taxonomy follows McKenna and Bell (1997). Measurements of teeth were made using an Ultra-Cal Mark III digital caliper.

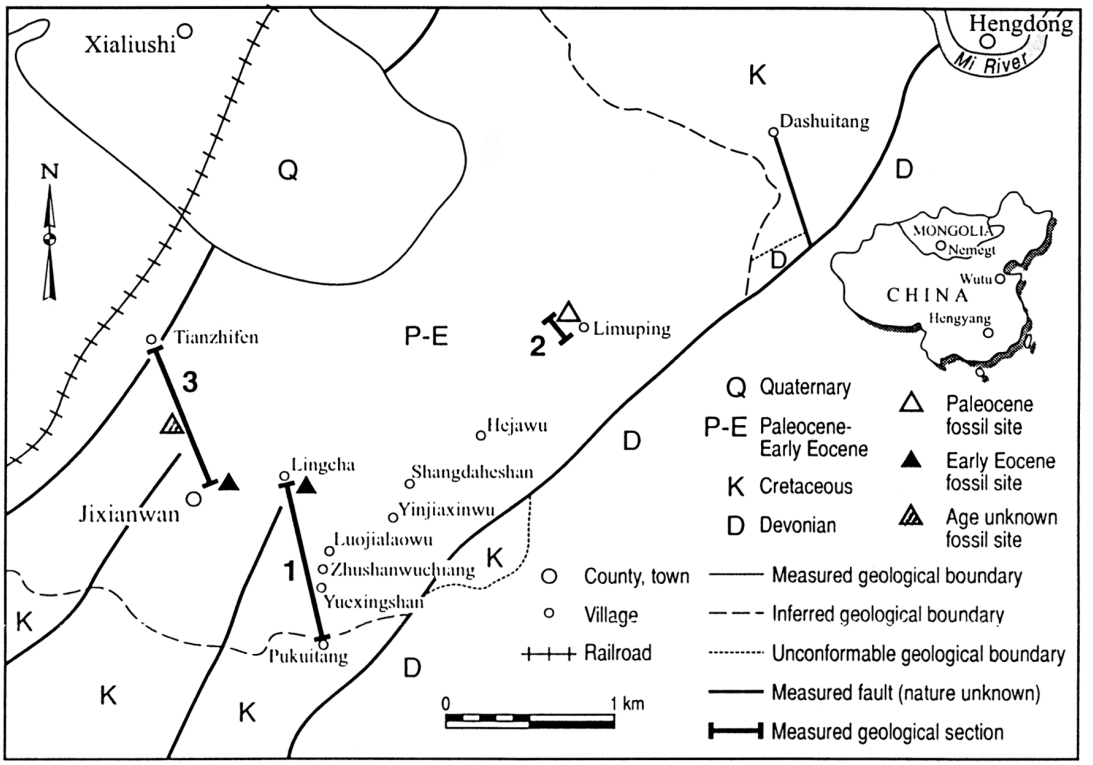

Fig. 1. Location map of early Eocene localities where specimens of *Matutinia* were collected.

SYSTEMATIC PALEONTOLOGY

MAMMALIA LINNAEUS, 1758

SIMPLICIDENTATA WEBER, 1904

EURYMYLIDAE MATTHEW, GRANGER, AND SIMPSON, 1929

Matutinia nitidulus Li, Chiu, Yan, and Hsieh, 1979

Rhombomylus nitidulus Dashzeveg and Russell, 1988: 149.

REFERRED SPECIMENS: IVPP V7443, skull with left dentary; IVPP V7444, a subadult, broken skull with associated right dentary and partial postcranial skeleton; IVPP V7445, skull with right posterior portion damaged; IVPP V7446, skull with dentary; IVPP V7447, partial skull; IVPP V7448, partial skull; IVPP V7449, partial juvenile skull; IVPP V7450, complete skull that has been sectioned.

LOCALITY AND AGE: The materials were collected from two early Eocene sites at Lingcha and Jixianwan about 15 km southwest of Hengdong, in the northeastern part of the Hengyang Basin, Hunan Province, China (27°05′N, 112°57′E; fig. 1). The early Eocene Lingcha Formation here consists of purplish red mudstone interbedded with fine sandstone and yellowish green or light and dark gray mudstone (Young, 1944; Li et al., 1979; Ting, 1995).

REVISED DIAGNOSIS: Similar to *Rhombomylus* but different from other basal Glires in having distinct hypocone shelf on upper cheek teeth; complex zygoma with dorsal and ventral processes of jugal and antero- and posteroventral processes of maxilla; tympanic bulla well developed with laterally elongate external auditory meatus; and mastoid portion of petrosal inflated and filled with bony septa, forming posterior part of bulla and exposed on skull roof between squamosal and parietal. Differing from *Rhombomylus* in having cheek teeth relatively lower crowned; p3 single-rooted; partial vertical groove on lingual side of upper

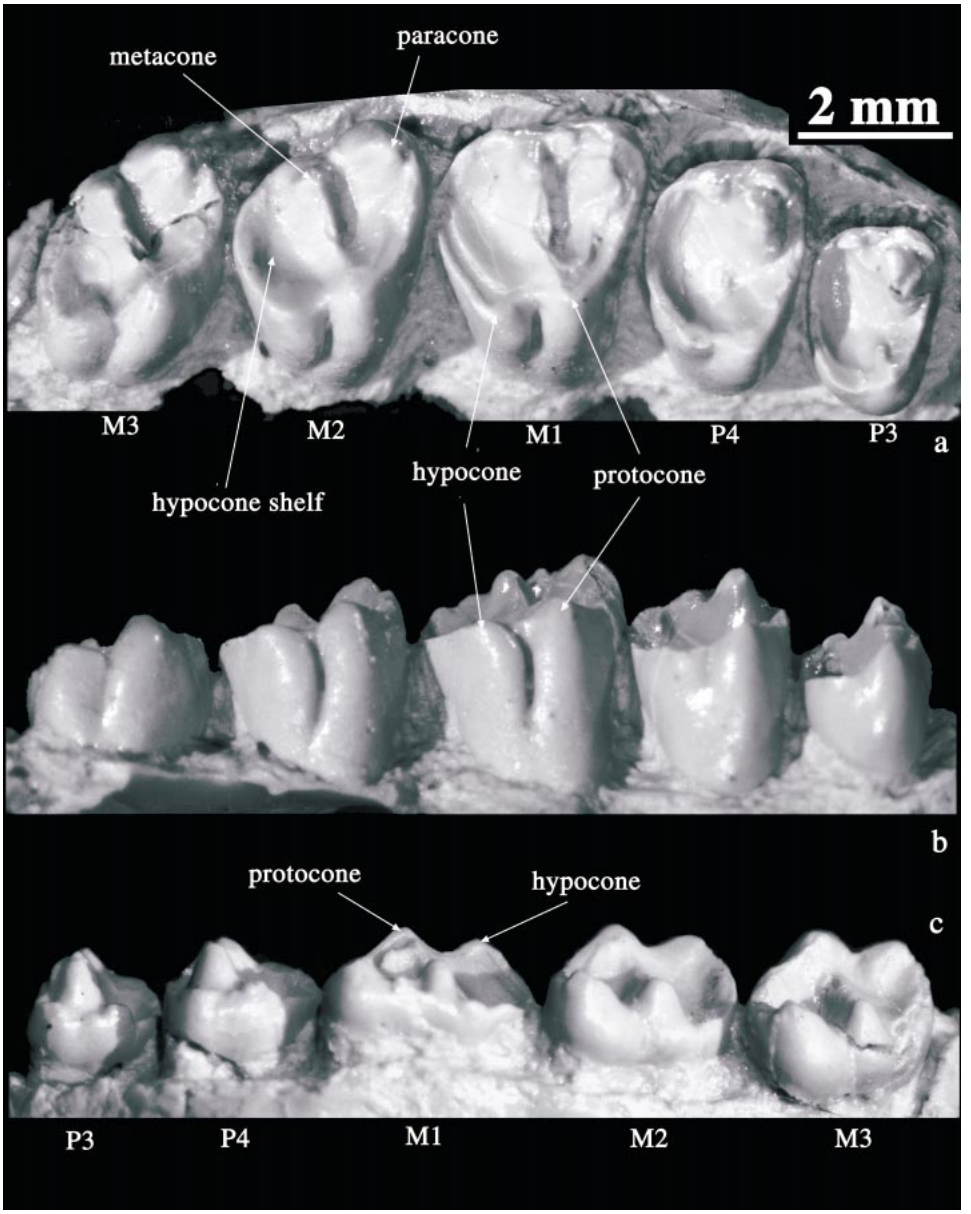

Fig. 2. **a–c,** Occlusal, lingual, and labial views of right upper cheek teeth (P3–M3, IVPP V7443) of *Matutinia nitidulus*.

cheek teeth; paracone and metacone more conical and more distantly separated; hypocone shelf relatively less well developed; shelf on M3 simple and small; ridges confining trigonid, cristid obliqua (ectolophid), and talonid cusps more distinct; smaller dorsal exposure of mastoid portion of petrosal; and separate carotid and stapedial foramina.

DESCRIPTION

UPPER DENTITION: The dental formula is 1-0-2-3/1-0-2-3. The lingual sides of the upper tooth rows are parallel, whereas the labial outlines of the tooth rows are convex (fig. 2). The incisors are well preserved in IVPP V7443 and IVPP V7446. As revealed by the

TABLE 1
Dental Dimensions of *Matutinia nitidulus* from Hengyang Basin, Hunan Province, China (length/width in mm)

IVPP no.	DP3	DP4	P3	P4	M1	M2	M3
V7443L			1.7/2.5	2.1/3.2	2.4/3.7		
V7443R			1.8/2.5	2.1/3.3	2.7/3.7	2.5/3.7	2.6/3.3
V7445L					2.5/3.7	2.6/3.6	
V7445R					2.8/3.9	2.6/3.6	
V7449L	1.5/1.7	1.8/2.9			2.7/3.7	2.5/3.4	
V7449R	1.5/1.7	1.9/3.1			2.6/3.7	2.5/3.3	
	dp3	dp4	p3	p4	m1	m2	m3
V7443L			1.7/1.3	2.2/2.0	2.9/2.2	3.1/2.5	
V7443R				2.3/2.1	3.0/2.3	3.0/2.5	3.3/2.4
V7449L	1.3/1.1	2.4/1.5			2.7/2.2	2.9/2.3	
V7445R		2.5/1.6			2.9/2.3	3.0/2.3	

breakage in the rostrum (IVPP V7444), the enlarged incisor extends posteriorly into the maxilla above the infraorbital foramen. The incisor grows through the premaxilla and bends ventrally and slightly posteriorly. The tips of the incisors contact each other. The thick enamel of the upper incisors covers the anterior surface of the teeth and wraps around the tooth laterally and medially. In IVPP V7443, the right incisor bears an elongate wear facet at the lingual side of the tip. The left incisor was apparently loosened from its alveolus, and its tip was broken.

The dP3 is preserved in the juvenile skull (IVPP V7449) in which the germ of the M3 is not yet formed. The tooth is small, triangular in crown outline, and has weak division of the paracone and metacone. The dP4 is molariform, bearing distinct cusps and a hypocone shelf, but has a lower crown than do the molars. Its paracone and metacone join the protocone by the paraloph and metaloph, forming a narrow V shape. P3 has one lingual and two labial roots. Its crown bears two cusps, the paracone and protocone, with the former being larger than the latter. The two cusps are connected anteriorly by a ridge, presumably the protoloph, that forms the anterior edge of the tooth and has a steep anterior surface. The ridge extends around the anterolateral corner of the paracone as a cingulum. A very small cusp at the posterolabial base of the paracone is probably the metacone. A hypocone is not present, but a broad hypocone shelf forms the posterior half of the tooth. The hypocone shelf is bordered posteriorly by a curved enamel ridge extending from the posterior base of the protocone to the metacone. A weak ridge extends posterolabially from the protocone and fades away before reaching the basin of the hypocone shelf. The enamel of the tooth wall is thick, but it is thin on the occlusal surface. P4 is generally similar to P3, but is distinctly larger than the latter (table 1; fig. 2).

All molars have three roots. The tooth crown is higher lingually than labially. M1 is the largest cheek tooth and is narrower lingually than labially (table 1; fig. 2). The protocone is triangular in occlusal view and columnar on its lingual surface in medial view. The paracone occupies the anterolabial corner of the tooth. The metacone is smaller and is slightly more lingual than the paracone. The two labial cusps are connected with the protocone by a strong protoloph and metaloph, defining a V-shaped trigon. Slight swelling at the middle part of the protoloph and metaloph, respectively, suggests a weak protoconule and metaconule. Unlike the premolars, the protoloph of M1 joins the paracone directly at its anterolingual base. A small mesostyle is between the paracone and metacone. There is no labial cingulum. The hypocone is lower and slightly more lingual than the protocone. On the lingual surface, a narrow, vertical groove separates the two cusps (fig. 2). The hypocone shelf, primarily formed by the postcingulum, is large and extends across the entire width of the posterior

half of the tooth. The most expanded region of the shelf is at, or labial to, the longitudinal axis of the tooth. As in the premolars, the enamel is thick in the vertical walls of the tooth, but it is thin on the crown surface. Moreover, the enamel decreases its thickness labially. The positions of wear facets on the lophs indicate that occlusion primarily involved crushing or grinding instead of shearing between teeth. M2 is smaller than M1; in particular, the width of the posterior half of the tooth is reduced. This trend of reduction is still greater in M3.

LOWER DENTITION: The single lower incisor extends posteriorly below the m3. The enamel covers the front surface of the tooth and extends laterally farther than that in the upper incisor. The dp3 and dp4 are preserved, but in poor condition, in IVPP V7449. The dp3 is small, whereas the dp4 is molariform. Its trigonid is not anteroposteriorly shortened. The talonid is fully developed and wider than the trigonid. It bears a hypoconid, entoconid, and hypoconulid.

The p3 is small, simple, and single-rooted (fig. 3). The main cusp is high and conical, being convex on the labial surface and concave on the lingual surface. In lateral view, the anterior surface of the tooth is gently convex. A short, low cingulum abuts the anterolingual base of the main cusp. The posterior surface of the main cusp bears a sharp ridge, which extends to the posterolingual base of the cusp. The talonid is about half the length of the trigonid and is much lower than the latter. The simple talonid is basically an oblique ridge, being separated from the main cusp by a transverse groove. Two small, weak cusps, presumably the hypoconid and the entoconid, are located on the labial and the lingual side of the ridge, respectively.

The p4 is double-rooted. Its trigonid is longer, higher, and wider than the talonid (fig. 3). The protoconid is the most prominent cusp of p4 and is connected to the metaconid by a curved ridge. The small paraconid is anterior to the metaconid. A cingulumlike anterior ridge extends from the paraconid to the anterior base of the protoconid. The height of the ridge decreases labially. Between the anterior ridge and the one connecting the protoconid and metaconid is a broad trigonid basin. Unlike in the molars, the protoconid of p4 does not have an anterior arm that forms the anterior edge of the tooth. The hypoconid and hypoconulid are near to each other on the labial side of the talonid. The hypoconid sends a low oblique crest to the middle of the posterior wall of the trigonid. A restricted talonid basin is formed lingual to the oblique crest.

Different from the upper molars, the lower molars increase in size posteriorly (table 1; fig. 3). The trigonid of m1 is anteroposteriorly short, about one-third the length of the tooth. The paraconid is absent. The protoconid sends an anterior and a posterior ridge to join the metaconid; the ridges define an oval, shallow, and transversely oriented trigonid basin. On the talonid, the hypoconid, hypoconulid, and entoconid are distinctive. The hypoconid is the largest talonid cusp, from which a strong cristid obliqua extends to the trigonid but is separated from the base of the trigonid by a narrow gap. There is no mesostylid. The hypoconulid is well separated from the hypoconid; both are connected by a low ridge. The hypolophid from the entoconid extends posterolabially to join the hypoconulid. The hypoconulid bears a ridge that extends lingually to the posterior base of the entoconid and forms the posterior edge of the tooth. The talonid basin is deep.

The m2 is larger than the m1. In relation to the talonid, the trigonid of m2 is relatively wider and shorter than are those of m1. The talonid is generally similar to that of m1, except that the cusps and ridges are more robust. The m3 differs from m1 and m2 in having a narrower but longer talonid, owing to the posterior extension of the hypoconulid. In IVPP V7449, which is little worn, the hypoconulid is divided into two closely paired cusps. The enamel of all cheek teeth is thicker labially than lingually.

ROSTRUM OF SKULL: The rostrum is rodentlike (figs. 4–6). The nasal is elongate, slightly flared at the anterior extremity of the snout, and even in width in the remainder (figs. 4, 6). It contacts the premaxilla laterally and the frontal posteriorly. In dorsal view, the length of the nasal is about one third of the skull length. The anterior process of the nasal extends slightly anterior to the upper incisor, marking the anterior extremity of the skull. The tips of the nasals slightly bend

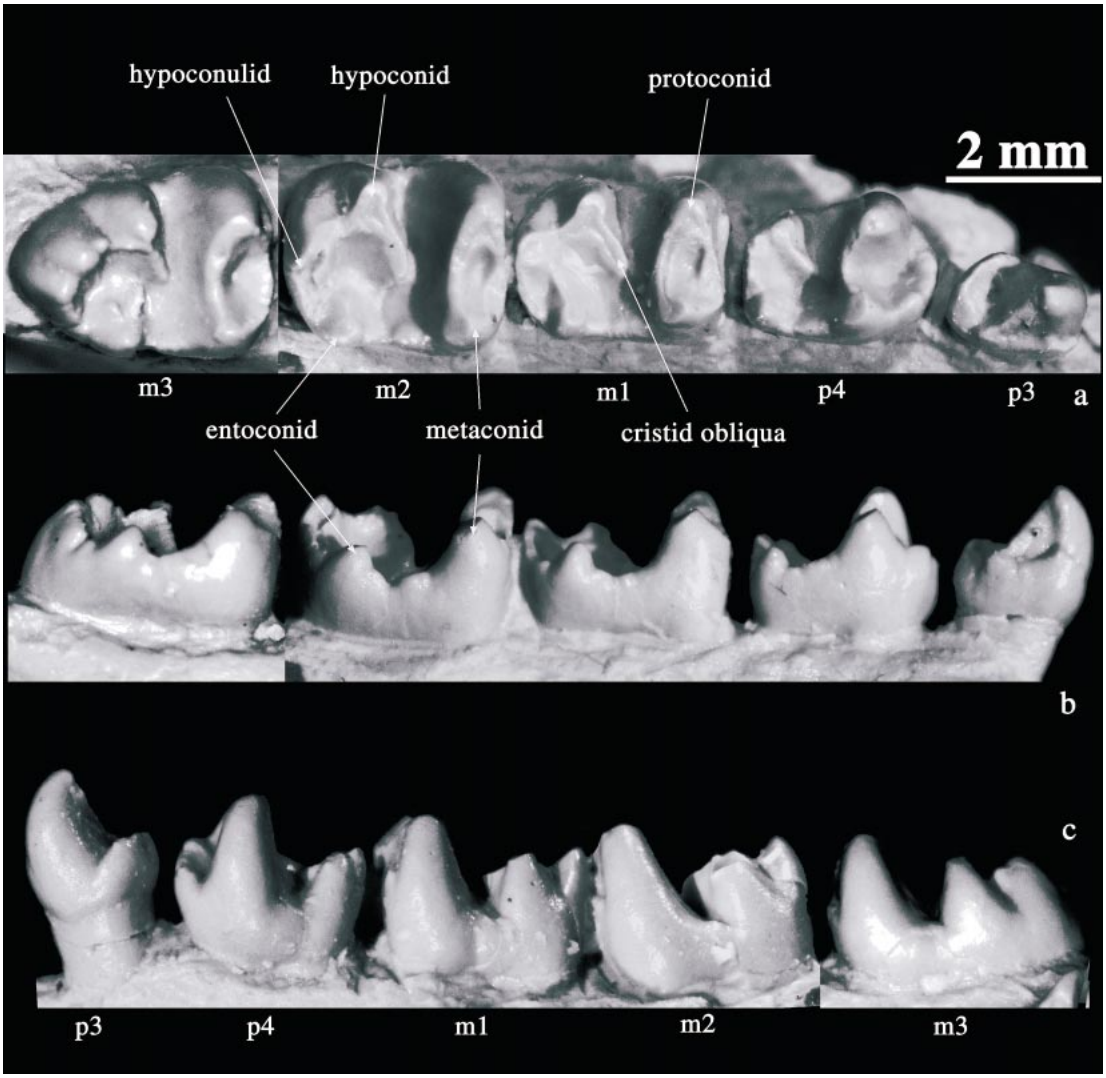

Fig. 3. **a–c,** Occlusal, lingual, and labial views of left lower cheek teeth (p3–m3, IVPP V7443) of *Matutinia nitidulus*. The m3 is photographically reversed from an image of the right m3 of IVPP V7443.

ventrally. The posterior border of the nasal is intruded by a triangular anterior process of the frontal; the posterior tip of the nasal reaches the level of the mid-point of the orbital rim.

The size and shape of the nasals of *Matutinia nitidulus* are similar to those of *Rhombomylus* (Li and Ting, 1985), although the posterior process of the nasal in *M. nitidulus* extends more posteriorly than it does in *Rhombomylus*. The nasal of *Heomys* is also large, but it differs from those of *Rhombomylus* and *Matutinia* in having a contraction at the level of the infraorbital foramen (Li, 1977).

The premaxilla is large, with an extensive posterior process and palatine process (figs. 4–6). It contains the enlarged incisor and contacts with the nasal dorsally, the frontal posteriorly, and the maxilla lateroventrally. It forms more than half of the lateral surface of the rostrum (fig. 6). The posterior process of

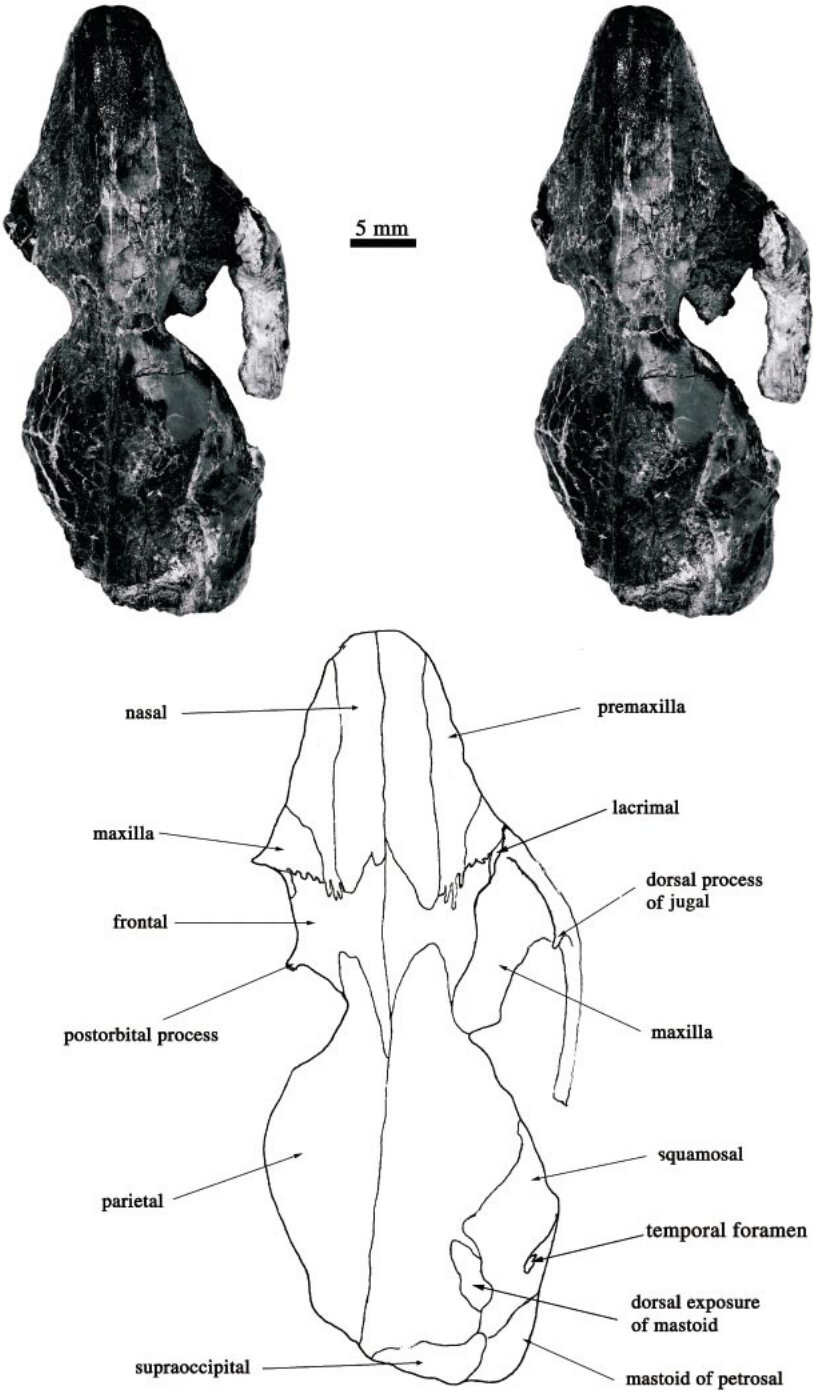

Fig. 4. Dorsal view of the skull of *Matutinia nitidulus* (IVPP V7443).

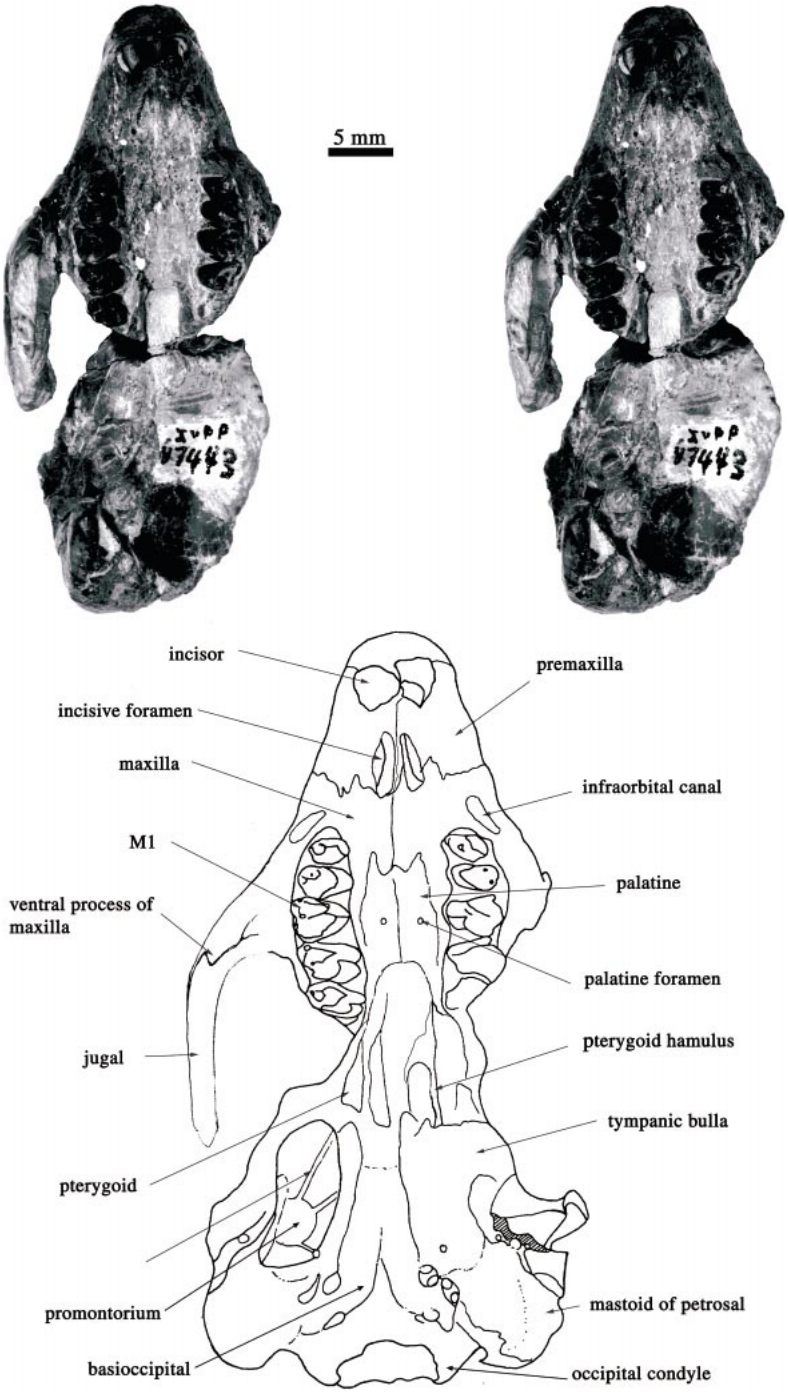

Fig. 5. Ventral view of the skull of *Matutinia nitidulus* (IVPP V7443). The line drawing reconstruction of the basicranial region is partly based on IVPP V7444.

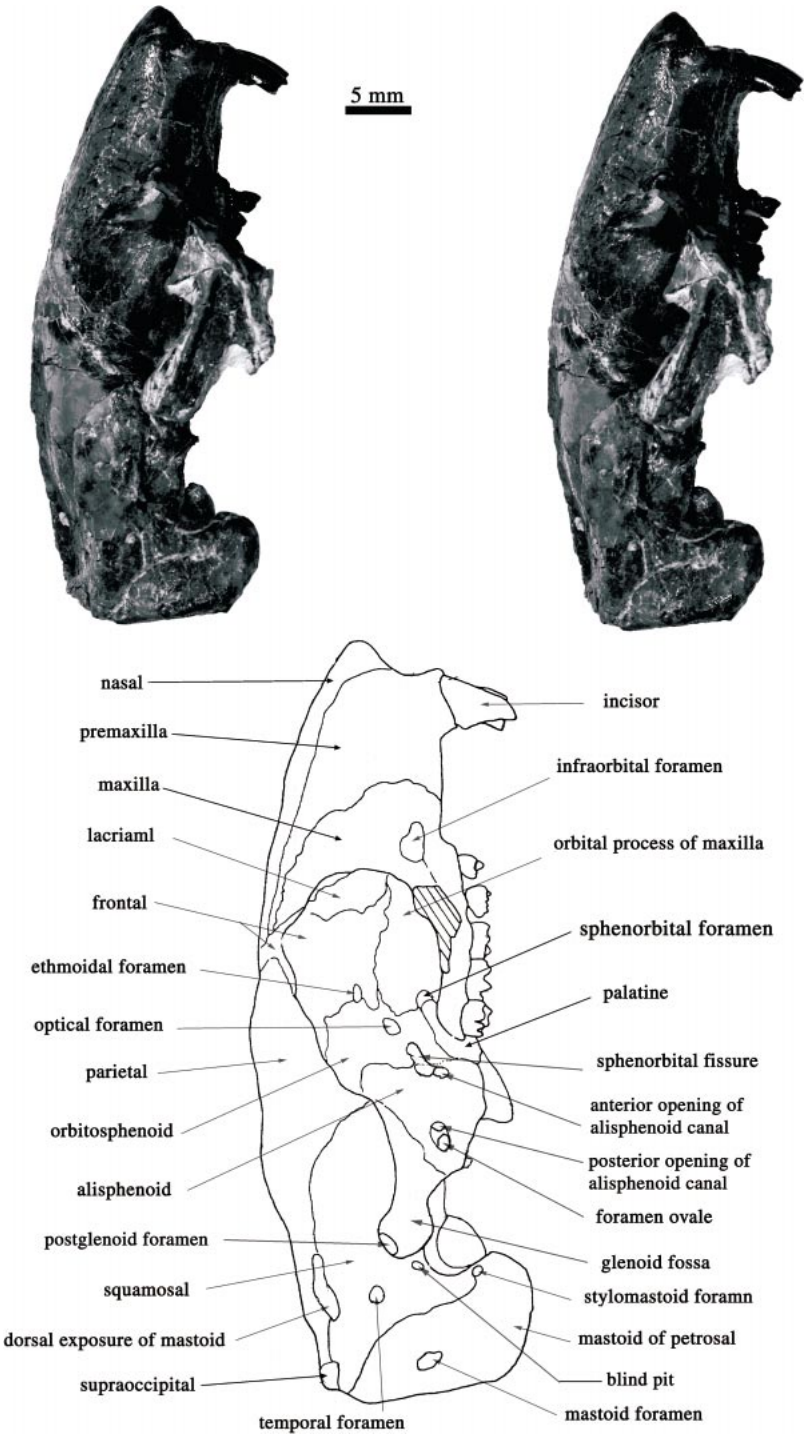

Fig. 6. Lateral view of the skull of *Matutinia nitidulus* (IVPP V7443). The zygomatic arch was removed in the drawing to reveal the orbital region.

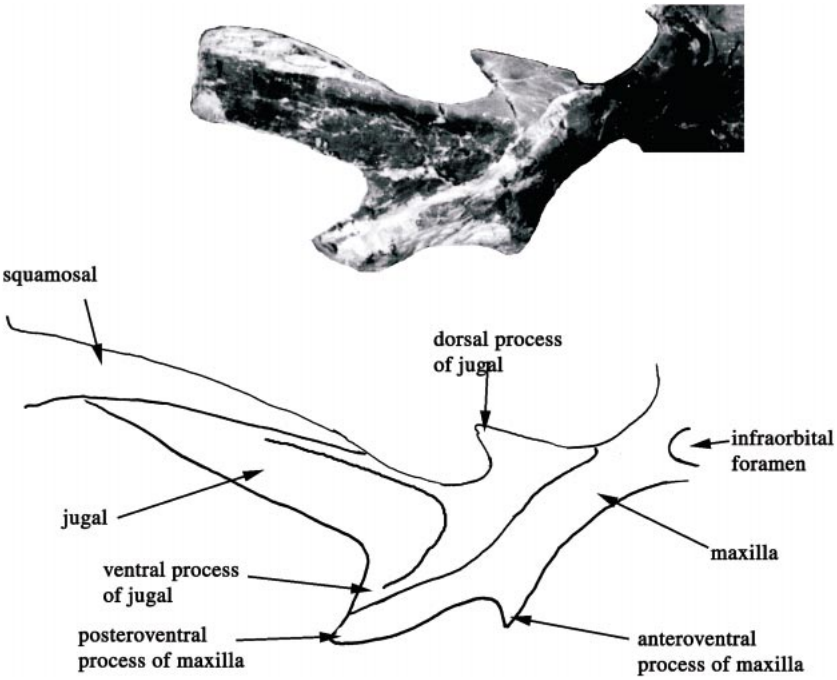

Fig. 7. Lateral view of the zygomatic arch of *Matutinia nitidulus* (IVPP V7443) and its reconstruction.

the premaxilla extends posterodorsally to the same level of the posterior tip of the nasal on the dorsal surface of the skull, where it meets the frontal in an interdigitated suture (fig. 4). The posterior process of the premaxilla completely separates the nasal from the maxilla. The palatal process of the premaxilla floors the anterior half of the nasal cavity. The premaxillary–maxillary suture runs perpendicular to the longitudinal axis of the skull, passing through the posterior edge of the incisive foramen, so that the premaxilla forms most of the lateral wall of the incisive foramen. The oval incisive foramina are anteroposteriorly elongate and anteriorly tapered. The mid-division of the incisive foramina is formed primarily by the premaxilla, which is more dorsally located than the surface of the palate; therefore, the entire area of the incisive foramina is dorsally concave.

A large premaxilla bearing an elongate posterior process and accommodating the enlarged incisive foramen is a common feature in Glires. Lateral fenestrations of the premaxilla and maxilla are absent in *Rhombomylus*, *Matutinia*, and *Heomys*, but are probably present in *Eurymylus* (Wood, 1942).

The maxilla is a large, complex bone (figs. 4–6). It narrowly contacts both the frontal and lacrimal on the facial region. The infraorbital foramen is oval, wider than high (2.2 $\times$ 1.4 mm), and located above the anterior edge of P3. A small depression extends anteriorly from the foramen. The infraorbital canal is short. It opens posteriorly within the orbit at the level of the posterior edge of P3. The posterior edge of the zygomatic process is situated at the level between M1 and M2. The zygomatic process is long and extends posteroventrally, forming the anteroventral portion of the zygoma. It has an extensive suture with a large jugal and bears two processes (fig. 7). The posteroventral process projects posteroventrally and is stronger than the anteroventral one, which extends ventrally.

Within the orbit, the maxilla makes up the entire floor, in which ends of cheek teeth roots are exposed. The large orbital wing of the maxilla extends to the mid-height of the orbital wall and has a broad contact with the

frontal dorsally. The maxillary-lacrimal suture is well defined at the anterior root of the zygomatic process. Posteriorly, the maxilla contacts the orbitosphenoid. The maxillary-orbitosphenoid suture runs along the medial wall of the orbit. A large sphenopalatine foramen is situated dorsal to the M3 at the junction of the orbitosphenoid, palatine, and maxilla (fig. 6). In palatine view, the maxilla forms the mid-portion of the palate between the premaxilla and palatine. The maxillary-palatine suture runs from the posterior edge of the palate, following the medial edge of the tooth row to the level of P3. The anterior portion of the suture is uneven.

Compared to the condition of *Matutinia*, the palatine process of the maxilla in *Heomys* is large and occupies about half of the palate. The maxillary-palatine suture of *Heomys orientalis* is at the level between P4 and M1, more posteriorly situated than that of *Matutinia*. *Matutinia* and *Rhombomylus* are similar in having the ventral projections of the zygomatic process of the maxilla. This condition is not seen in any early Glires in which the zygomatic arch is preserved. These processes may contribute to the attachment of the jaw muscles and probably function for incisive gnawing.

ORBITAL REGION OF SKULL: The lacrimal (figs. 4, 6) has a narrow band exposed on the facial region and a sizable orbital portion that frames the anteromedial corner of the orbit but does not contribute to the roof of the infraorbital canal. It contacts the maxilla anteriorly and ventrally, and the frontal posteriorly. The lacrimal-frontal suture runs from the lateral end of the frontal-maxillary suture ventrally to the anteroventral corner of the orbit. The lacrimal foramen is large and circular, located at the anterior edge of the bone. The lacrimal of *Matutinia* is similar to that of *Rhombomylus* in both size and shape.

The flat frontal is short in the skull roof (fig. 4). The medial part of the frontal projects both anteriorly and posteriorly as triangular processes. The body of the frontal is intruded upon by the nasal anteriorly and by the parietal posteriorly. The shortest area of the frontal is thus between the projected tips of the nasal and parietal. Lateral to this short region, the frontal expands to form a wing-shaped plate that borders the dorsal rim of the orbit laterally. No foramen is present in the frontal at this region. A short crescentic ridge on the lateral edge of the frontal, posterior to the frontal-maxillary suture, is considered to be the supraorbital crest. The prominent postorbital process is located at the posterior end of the supraorbital crest and projects posterolaterally. The process is broken in our specimens, but it did not connect with the dorsal process of the jugal to close the orbit posteriorly. Posterior to the postorbital process, the skull roof is considerably constricted, forming the narrowest region of the skull. The large orbital process of the frontal forms the dorsal half of the medial orbital wall (fig. 6). The crescent-shaped ethmoid foramen is at the middle of the frontal-orbitosphenoid suture. The frontal of *Matutinia* is similar to that of *Rhombomylus* in its shape, size, and relationships with surrounding elements.

The jugal is prominent, making up the main and central part of the zygomatic arch (figs. 6, 7). Anteriorly, it overlaps the maxilla but does not contact the lacrimal. The body of the jugal is deep and possesses dorsal and ventral processes. The dorsal process projects posterodorsally and forms the posterior half of the ventral rim of the orbit. The ventral process of the jugal and the posteroventral process of the maxilla form a strong, hook-like posteroventral projection of the zygomatic arch. The body of the jugal gradually tapers posteriorly and is overlapped dorsally by the zygomatic process of the squamosal. On the lateral surface of the jugal there is a ridge along the upper edge of the body. Ventral to the ridge is a broad, concave area that apparently serves for attachment of the jaw muscles. The jugal of *Matutinia* is similar to that of *Rhombomylus* in both size and shape.

POSTORBITAL REGION OF SKULL: The parietal is a long bone, extending more than half of the skull length (figs. 4, 6). It has broad contacts with the frontal anteriorly, the squamosal laterally, and the supraoccipital posteriorly; its contact with the squamosal is the most extensive of the three. The anterior part of the parietal is smooth and convex, whereas the posterior half becomes flat or slightly concave. The sagittal crest is moderate in height, starting at the area where the posterior process of the frontal intrudes the pari-

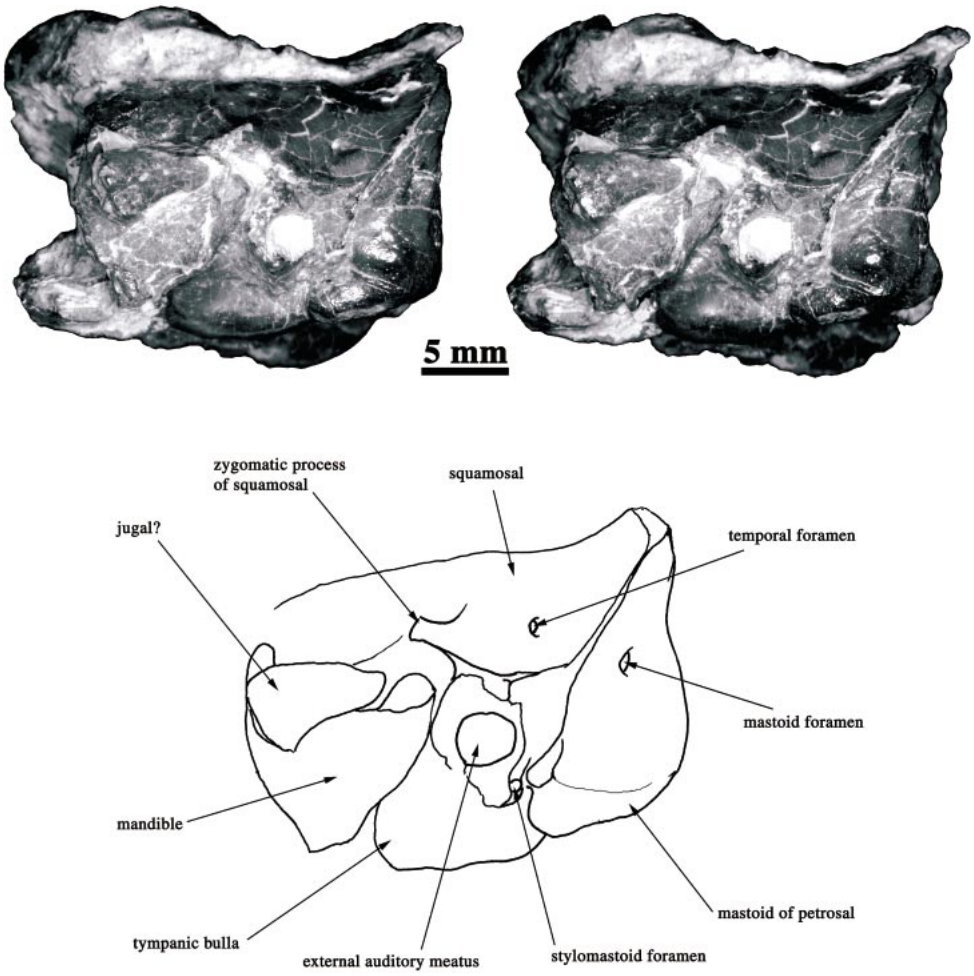

Fig. 8. Lateral view of the temporal and ear regions of *Matutinia nitidulus* (IVPP V7444).

etal (fig. 4). The parietal–squamosal suture is smooth and extends across the temporal region of the skull to meet the supraoccipital posteriorly. A small portion of the mastoid of the petrosal is exposed between the posterior parts of the parietal and squamosal. The parietal–alisphenoid contact is narrow and marks the ventralmost extension of the parietal in the temporal region. The parietal of *Matutinia* is similar to that of *Rhombomylus*; the dorsal exposure of the petrosal, however, is smaller than that in *Rhombomylus*.

The squamosal covers most of the temporal region of the skull (figs. 4–6, 8, 9). In this region the squamosal contacts the parietal dorsally, the alisphenoid anterolaterally, and the mastoid of the petrosal dorsally and posterolaterally. A single temporal foramen occurs in the squamosal lateral to the dorsal exposure of the petrosal and anterior to the squamosal-mastoid suture. There is a depression, shaped like a foramen externally, between the upper rim of the external acoustic meatus and the lateral edge of the squamosal. The squamosal–mastoid suture follows a blunt ridge, which is a lateral extension of the lambdoidal crest, to border the posterior border of the skull. In ventral view, the glenoid fossa is a narrow trough oriented anteroposteriorly. There is no postglenoid process. A long, bony external auditory meatus, however, blocks the glenoid fossa posteriorly and may function as the postglenoid process. The

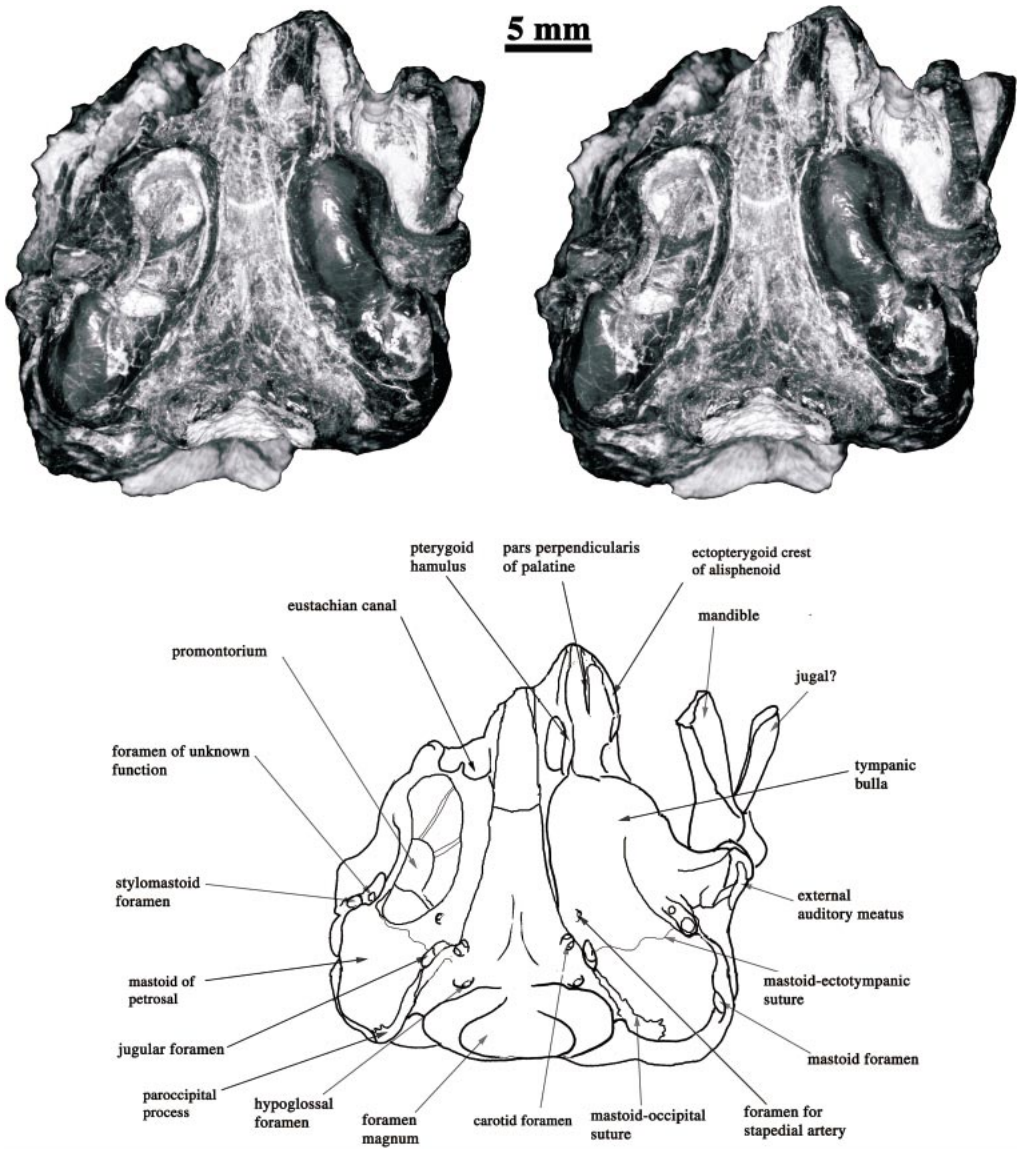

Fig. 9. Ventral view of the basicranium of *Matutinia nitidulus* (IVPP V7444).

large postglenoid foramen is at the posteromedial corner of the glenoid fossa. Because the glenoid fossa anterior to the external auditory meatus is deeply notched, a blood vessel could pass through the postglenoid foramen from the lateral side of the glenoid fossa without being pressed by the mandibular condyle. Anterolateral to the glenoid fossa is the zygomatic process of the squamosal, which extends anteriorly and overlaps the dorsal side of the jugal (figs. 6, 7). Because of breakage, the exact length of the process cannot be determined. A ventral process inserts between the expanded mastoid of the petrosal and the external auditory meatus.

The squamosal of *Matutinia* is similar to that of *Rhombomylus*, particularly regarding the position of the postglenoid foramen. This condition differs from that of other mammals in which the foramen is posterior to the postglenoid process. In rodents, this foramen is on the lateral side of the squamosal and is

posteromedial to the glenoid fossa (Wahlert, 1974).

The alisphenoid is a large, obliquely square bone, forming the sloping posterior wall of the orbitotemporal fossa (figs. 6, 9). It contacts the parietal posterodorsally, the squamosal posteriorly, the orbitosphenoid anteriorly, and the palatine anteroventrally. The alisphenoid-orbisphenoid suture lies at the posterior rim of the medial wall of the orbit and is anteroposteriorly oblique. The alisphenoid–palatine suture is short, connecting the orbitosphenoid-palatine suture at the posterior edge of the palatine. Several foramina are related to the alisphenoid. The sphenorbital fissure is posteroventral to the optic foramen and is partially obscured by cracks in IVPP V7443. There is a round foramen of unknown function on the anterior wall of the sphenorbital fissure. The orbitosphenoid contributes partly to the medial wall of the fissure. A large foramen lateral to the sphenorbital fissure and separated from the latter by a thin bony septum is the anterior opening of the alisphenoidal canal. Posterior to the anterior opening of the alisphenoidal canal is a large depression in which there are two foramina (fig. 6). The anterior one is the posterior opening of the alisphenoidal canal, and the posterior one is the foramen ovale. Separated by the lateral branch of the pterygoid from the dorsal opening is the foramen ovale accessorius (Wahlert, 1974). This foramen is situated horizontally and faces downward. The ventralmost part of the alisphenoid is a bony plate that forms the ectopterygoid crest lateral to the pterygoid. The posterior part of the plate contacts the anterolateral side of the bulla, but does not contribute to the bulla.

The orbitosphenoid is an elongate, narrow, rectangular bone lying on the posteromedial wall of the orbit (fig. 6). It contacts the frontal and the maxilla anteriorly, the alisphenoid posteriorly, and the palatine ventrally. A large, circular optic foramen is in the center of the orbitosphenoid.

The sutures of the pterygoid with the alisphenoid and presphenoid are fused, so that the boundaries are difficult to identify (figs. 5, 6, 9). A crack between the posterior edge of the palatine and the anterior edge of the pterygoid probably is coincident with the palatine-pterygoid suture in IVPP V7443. The ectopterygoid fossa is defined by the ectopterygoid crest of the alisphenoid laterally and by the entopterygoid crest of the pterygoid medially. The entopterygoid crest of the pterygoid forms the posterior part of the lateral wall of the choana and continues posteriorly as a slim hamulus that contacts the anteromedial corner of the bulla. The pterygoid hamulus thus confines a hollow space above it. An unusual feature in the pterygoid region of *Rhombomylus* is that the pars perpendicularis of the palatine continues posteriorly as another bony process that divides the ectopterygoid fossa longitudinally. A similar process is present in *Matutinia* (fig. 9), although its origin is not certain because of breakage. Nonetheless, we tentatively identify that process as the pars perpendicularis of the palatine. The pterygoid of *Matutinia* is similar to that of *Rhombomylus* in having the connection between the hamulus and the tympanic bulla.

The palatal process of the palatine occupies about a third of the hard palate (figs. 5, 6). It contacts the maxilla laterally and anteriorly, and the pterygoid posteriorly. The posterior rim of the palatine is formed by a blunt ridge, the postpalatine torus, and does not bear a postpalatine spine. In each palatal process, there are two palatine foramina. The anterior palatine foramen is medial to the posterior edge of P4 and the posterior one opposite to the posterior edge of M1. Fine grooves lead from these foramina anteriorly. The orbital process of the palatine is small, located at the posteroventral corner of the orbit. It contacts the maxilla anteriorly, the orbitosphenoid dorsally, the alisphenoid posteriorly, and the pterygoid posterolaterally. The shape and the proportion of the palatine of *Matutinia* are similar to those of *Rhombomylus*.

The sphenoid complex is best seen in IVPP V7444 (fig. 9). The sphenoid is a narrow splint of bone that gradually decreases in width anteriorly. The anterior contact of the sphenoid with other elements is not clear because of breakage. It contacts the pterygoid anteriorly and the tympanic bulla posteriorly. The sphenoid-basioccipital suture is short but distinct, situated between the anterior corners of the tympanic bullae. The ventral surface of the sphenoid is smooth.

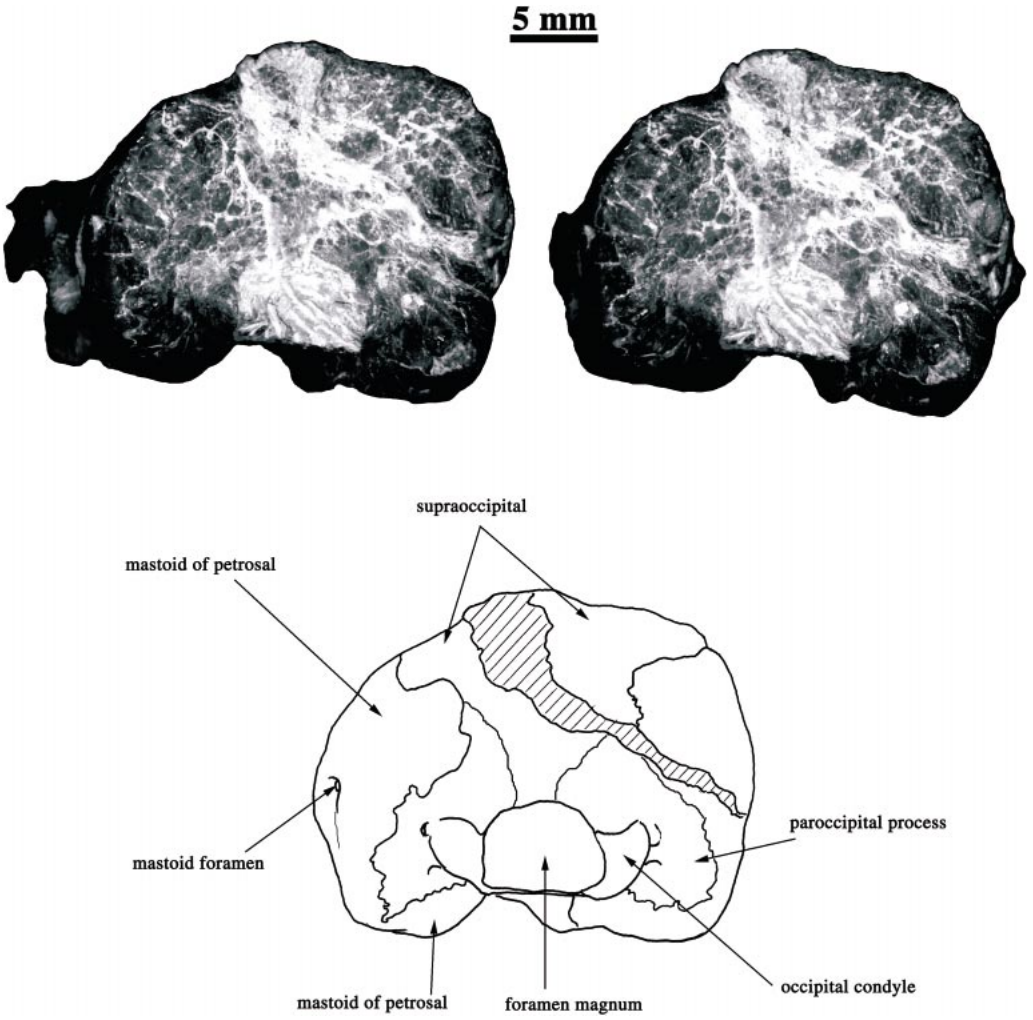

Fig. 10. Occipital view of *Matutinia nitidulus* (IVPP V7444).

OCCIPITAL REGION OF SKULL: The occipitals, including the basioccipital, the supraoccipital, and the exoccipital, are all well preserved in IVPP V7444 (figs. 9, 10); the dorsal part of the supraoccipital is also present in IVPP V7443 (fig. 4). In ventral view, the basioccipital is a large element, extending anteriorly as shown by the position of the sphenoid-basioccipital suture. It is somewhat trapezoidal, narrower anteriorly. A low keel extends along the longitudinal axis on the ventral surface of the basioccipital, on both sides of which the basioccipital is concave. The anterior portion of the basioccipital contacts the tympanic bulla laterally, forming a smooth, slightly curved suture. The posterolateral corner of the basioccipital joins the paroccipital process in a trough defined by the occipital condyle medially and by the mastoid process of the petrosal laterally. The jugular foramen is slitlike and walled by the ectotympanic anteriorly and the mastoid posteriorly; it is medially bounded by a ventral lip from the basioccipital. Anteromedial to the jugular foramen is the carotid foramen. This foramen is circular and is primarily surrounded by the basioccipital, with only a small contribution of the ectotympanic at its anterolateral corner. The foramen bifurcates into foramina of unequal sizes; the major one

courses anteriorly, whereas the minor one extends dorsolaterally, probably into the braincase.

The occipital condyle is low. The crescentic hypoglossal foramen occurs anterior to the ventral lobe of the condyle (fig. 9). More deeply, the foramen diverges into two smaller foramina, with the medial one being larger than the lateral one. The suture between the paroccipital of the occipital and the mastoid portion of the petrosal is definite; it starts from the posterior corner of the jugular foramen, runs ventrally, and then turns around to the occipital region. As indicated by the suture, the paroccipital process forms the posteromedial corner of the bullalike structure, most of which is the inflated mastoid of the petrosal.

In occipital view, the paroccipital-mastoid suture courses dorsally to the lambdoid crest (fig. 10). The supraoccipital is fan-shaped, with its dorsal edge forming the main part of the lambdoid crest. This crest is sharp and projects posterodorsally. A narrow band of the supraoccipital is exposed on the dorsal side of the crest. The foramen magnum is relatively small in occipital view and oval, with the long axis transverse. The dorsal lobe of the occipital condyle extends posterior to the level of the foramen magnum.

The occipital of *Matutinia* is similar to that of *Rhombomylus*, but the lambdoid crest of *Matutinia*, as shown in IVPP V7444, appears stronger than that of *Rhombomylus*. The paroccipital process in *Rhombomylus* forms a protuberance. Most notable in this region is absence of the carotid foramen in *Rhombomylus*.

AUDITORY REGION OF SKULL: The auditory region is characterized by a large ectotympanic bulla and the greatly inflated mastoid process of the petrosal, as is best seen in IVPP V7444 (figs. 8, 9). Although the two elements together form a continuous bean-shaped structure, the suture between them is definite. We do not regard the inflated mastoid as part of the bulla because the chamber of the inflated mastoid is filled with septa and the entire region is posterior to the middle tympanic cavity in which the promontorium and ear ossicles are located. However, the partitioned space of the mastoid is confluent with the tympanic cavity through an opening at the ectotympanic-mastoid suture.

Although the bulla is delimited from the alisphenoid, basioccipital, and squamosal by sutures, there is no suture on the bulla proper; therefore, we consider the bulla to be exclusively ectotympanic. The bulla completely covers the tympanic cavity. Its medial portion is smooth and gently rounded, whereas the lateral side is irregular and extends laterally as the external auditory meatus. The meatus is long, with the anterior wall being longer than the posterior one, so that the opening of the meatus faces posterodorsally. The anterior wall of the auditory meatus also functions as the postglenoid process, which extends laterally across the full width of the glenoid fossa. The dorsal tip of the meatus reaches the lateral ridge of the squamosal. The ventral side of the external auditory meatus is ridgelike. Between the meatus and the inflated mastoid of the petrosal is a transverse trough in which there are two foramina. The lateral, larger one is the stylomastoid foramen, which can be traced into the tympanic cavity from the breakage of the ear region in IVPP V7443. The stylomastoid foramen is for passage of the facial nerve that was enclosed in a bony tube in the middle tympanic cavity. The medial foramen is smaller, and its identification is uncertain. At the anterior end of the bulla and dorsal to the hamulus-bulla contact, the eustachian canal opens anteriorly. On the posteromedial side of the bulla there is a small foramen, which is identified as the foramen for the stapedial artery (fig. 11). Viewed from the breakage in the right ear of IVPP V7444, the foramen penetrates the medial wall of the tympanic bulla. However, because the foramen is small, whether it contained a functional stapedial artery is uncertain. Inside the bulla, there is no bony septum except the one that connects the promontorium and the foramen for the stapedial artery. This bony septum is deep and vertical; it probably supported a bony tube containing the stapedial artery, if a functional stapedial artery existed. There are two other ridges extending from the promontorium anteromedially on the roof of the tympanic cavity; these are of petrosal origin (fig. 11). The bony ring for attachment of the tympanic membrane is circular with a di-

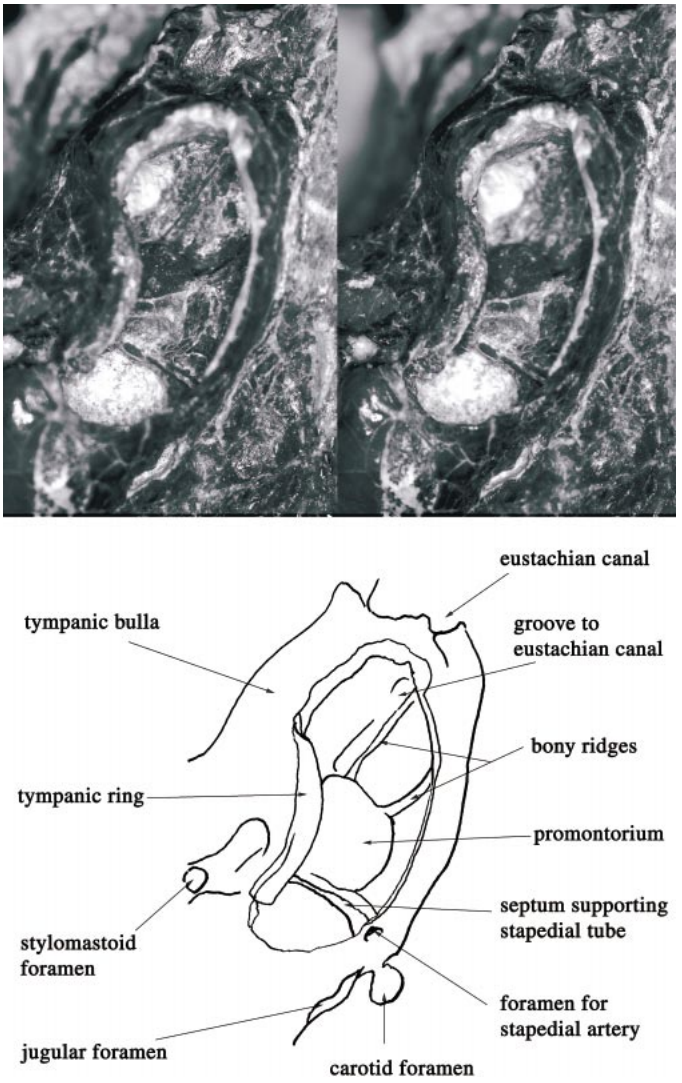

Fig. 11. Left ear region of *Matutinia nitidulus* (IVPP V7444), with bullar wall broken.

ameter of approximately 4 mm; it can be seen in the right tympanic bulla. The ring is inclined with the medial plane facing dorsomedially. The inclination has a high angle to the horizontal plane of the skull, but measurement of the degree is difficult.

The mastoid of the petrosal has expanded significantly (figs. 4–6, 8–10). It is no longer a processlike structure as in many other eutherian mammals; it is a hollow shell with a rounded external surface. The suture between the ectotympanic bulla and the mastoid is clear. It starts from the medial wall for the jugular foramen, extends transversely, and ends in the trough that holds the stylomastoid foramen. The chamber of the inflated mastoid is filled with numerous thin bony septa, which divide the chamber into cells (or sinuses). The chamber is confluent with the middle tympanic cavity through an opening posterior to the fenestra cochleae. In lateral view, the mastoid of the petrosal forms the posterior end of the skull posterior to the squamosal–mastoid suture. The exposure of the mastoid in this region has a convex surface, which is broad ventrally. It gradually

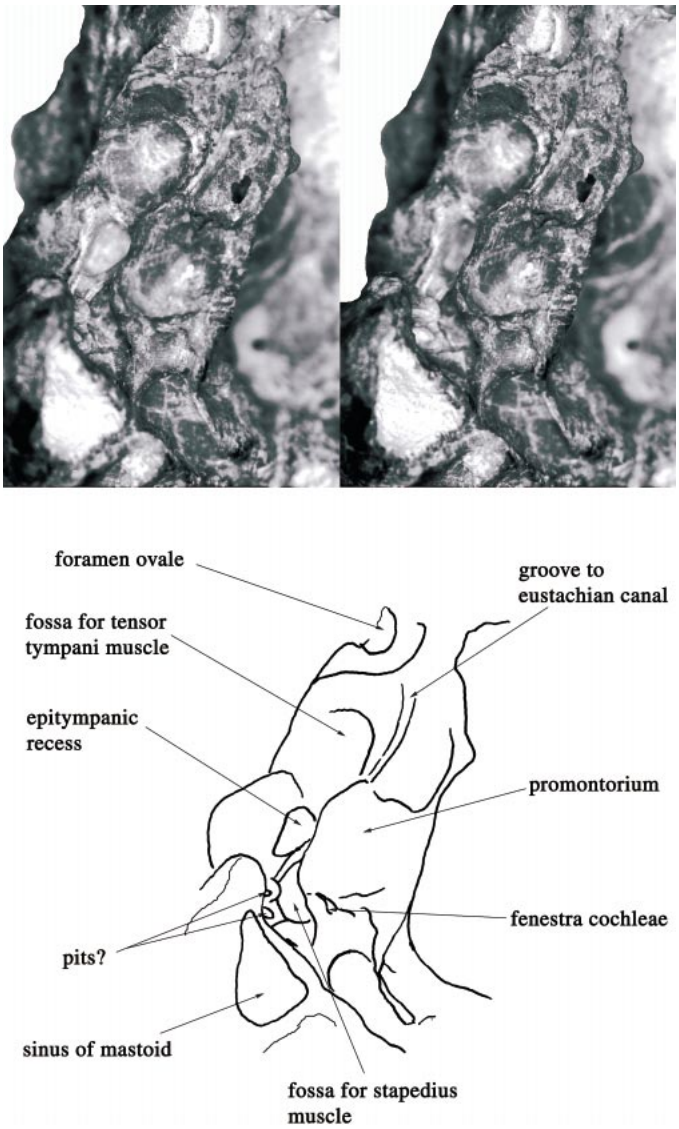

Fig. 12. Ventromedial view of the right petrosal of *Matutinia nitidulus* (IVPP V7443).

thins dorsally to merge into the lambdoid crest. At about the level of the dorsal rim of the external auditory meatus, a mastoid foramen opens posterolaterally within the mastoid (fig. 6). The mastoid has an extensive exposure in the occipital aspect of the skull. Moreover, the dorsal extension of the mastoid penetrates the skull roof dorsally and is exposed between the parietal and squamosal.

The tympanic cavity is spacious and longitudinally elongate (figs. 11, 12). The promontorium is prominent, projected from the tympanic roof as a bulbous structure with a rounded ventral surface. It is broad posteriorly and narrow anteriorly. As mentioned above, a thin bony septum supporting the stapedial artery connects the posteromedial corner of the promontorium to the foramen. On the ventral rim of this septum is a small bony tube leading laterally from the stapedial foramen. Because of breakage, the lateral extension of this tube is not preserved. However, a narrow groove on the posterior rim of the promontorium suggests continuation of

the stapedial tube. The groove leads toward the fenestra vestibuli and is filled with matrix. At the anterolateral corner of the promontorium is a distinctive bony trough bounded by two short, bony septa. This trough runs from the anterior edge of the promontorium to the opening of the eustachian canal at the anteromedial corner of the bulla. The fenestra cochleae (best revealed in IVPP V7443) is dorsoventrally elongate and faces posteriorly. On the lateral wall of the promontorium and anterior to the posterior edge of the promontorium is the fenestra vestibuli. The precise size of this fenestra is unknown because of breakage.

Anterolateral to the promontorium, the fossa for the tensor tympani muscle is a sizable depression (fig. 12). Posterior to, and separated by a thin bony septum from, this fossa is a deep and triangular epitympanic recess. It can be inferred that the ear ossicles were suspended in this region in life. Dorsal and posterolateral to the fenestra vestibuli is a deep fossa for the origin of the stapedius muscle. The passage for the facial nerve is probably contained in a bony tube that forms part of the bony wall separating the fossa for the stapedius muscle and the epitympanic recess; the tube exits the tympanic cavity through the stylomastoid foramen. There are two small pits posterior to the epitympanic recess. These pits are filled with matrix; therefore, it cannot be seen whether they are depressions or foramina. The small, anterior one may be the exit for the stapedial artery.

Several distinct features are exposed on the intracranial surface of the petrosal in IVPP V7443 (fig. 13). The petrosal is extensive and forms the entire sidewall of the posterior braincase. At the dorsal edge, a large, oval fossa (or foramen) is filled with matrix. Whether this fossa is actually a foramen is uncertain. Ventral to this fossa, the subarcuate fossa is deep and circular, with a diameter of about 2 mm. The bone forming the rim of the subarcuate fossa is broken, revealing the space of the anterior semicircular canal. Anteroventral to the subarcuate fossa is the internal acoustic meatus. The meatus contains the foramen for the facial (VII) nerve anterodorsally and the foramen for the auditory (VIII) nerve posteroventrally. Posterior to the internal acoustic meatus is a fissurelike foramen for the aquaeductus cochleae.

The auditory region of *Matutinia* is similar to that of *Rhombomylus* (Ting and Li, 1984; Li and Ting, 1985), being characterized by an inflated mastoid. The inflated mastoid makes up the sidewall of the posterior braincase, is exposed in the roof of the skull, and forms a continuous bulbous shell with the bulla. *Matutinia* further differs from *Rhombomylus* primarily in retaining the carotid foramen, which is lost in *Rhombomylus* (see also Discussion).

POSTCRANIAL SKELETON: The morphology of the postcranial skeleton is based solely on IVPP V7444, which is a subadult with broken skull, associated right dentary, and partial postcranial skeleton. A fragmentary glenoid part of the scapula is preserved in articulation with the head of the humerus (fig. 14). The glenoid fossa is shallow and elliptical. The supraglenoid tubercule is blunt and short. The scapular spine is high. The infraspinous fossa is broad and deep near the glenoid region. Only proximal segments of humeri were available, so that the length of the humerus is unknown. The shaft is slightly curved, and the proximal end shows no expansion. In anterior view, the shaft is flat, showing no sign of an intertubercular groove, except for a shallow gap between the tuberosities. In lateral view, the deltopectoral crest is weak. The head of the humerus is subspherical. The greater tuberosity is larger and more proximal than the lesser tuberosity, but is less so than the head.

The distal ends of the left radius and ulna are preserved in articulation with the manus (fig. 15), although they may have been slightly twisted counterclockwise in relation to the proximal–distal axis of the manus. The distal end of the radius is robust, but the styloid process on the medial side is broken. The distal end of the ulna is at the ventrolateral side of the radius and bears a distinct styloid process. Detailed morphology of this region is not observable because of poor preservation.

The left manus is well preserved (fig. 15). Although the hand has been flexed ventrally, the wrist elements remain largely in their anatomical relationship. The proximal row of the carpus consists of three bones, from the

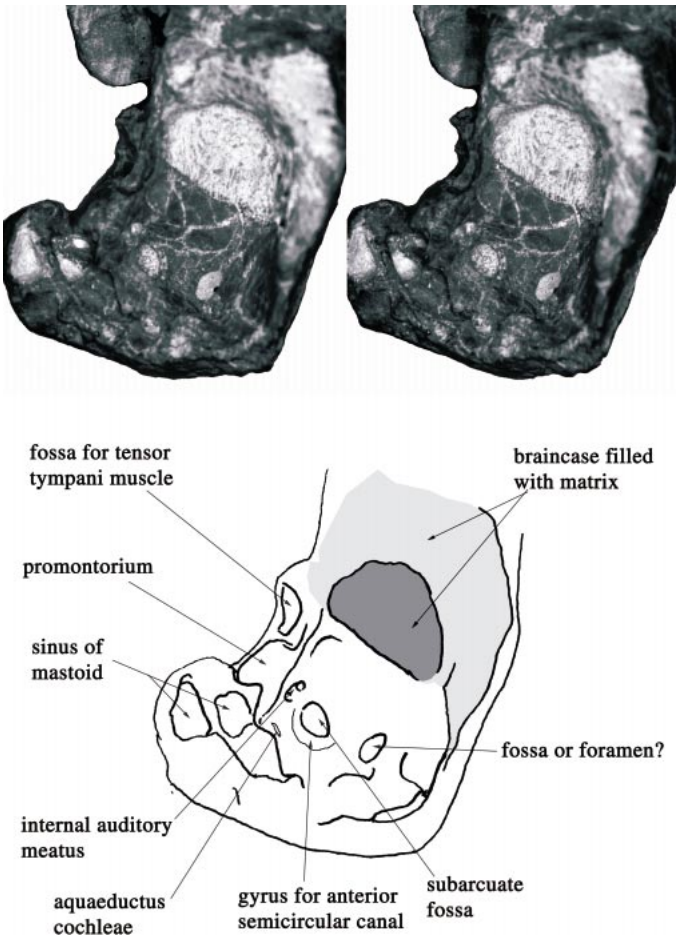

Fig. 13. Cranial view of the right petrosal of *Matutinia nitidulus* (IVPP V7443).

medial to the lateral, the scaphoid, lunar, and cuneiform. The scaphoid, the largest of the three, is transversely elongate in dorsal view. Proximally, the scaphoid articulates with the radius. As in other mammals, the scaphoid articulates distally with the trapezium medially and with the trapezoid, and probably the centrale, laterally. The lunar, the smallest of the three, appears to be pushed out slightly dorsally. The lunar contacts the radius proximally and the magnum distally. The anteromedial corner and the anterolateral corner of the lunar may also contact the centrale (fused with the trapezoid) and the unciform, respectively. Because the bone is displaced, these relationships are not observed in direct contact. The cuneiform is also transversely long, but less so than is the scaphoid. It articulates with the ulna proximally and with the unciform distally. On the ventral side, the cuneiform articulates with a large pisiform. The pisiform also contacts the ulna. The proximal end of the pisiform shows an elongate, saddle-shaped articular facet, whereas the distal end is expanded and knoblike; the expansions of the two ends of the pisiform are at right angles to each other.

The distal row of the carpus contains four elements. The medial one is the trapezium, which is roughly pentagonal in dorsal view. It articulates with the first metacarpal distolaterally. The second bone in the row has a complex shape; its medial part articulates with the second metacarpal distally. The lateral part projects dorsally as a process and contacts the scaphoid and lunar proximally.

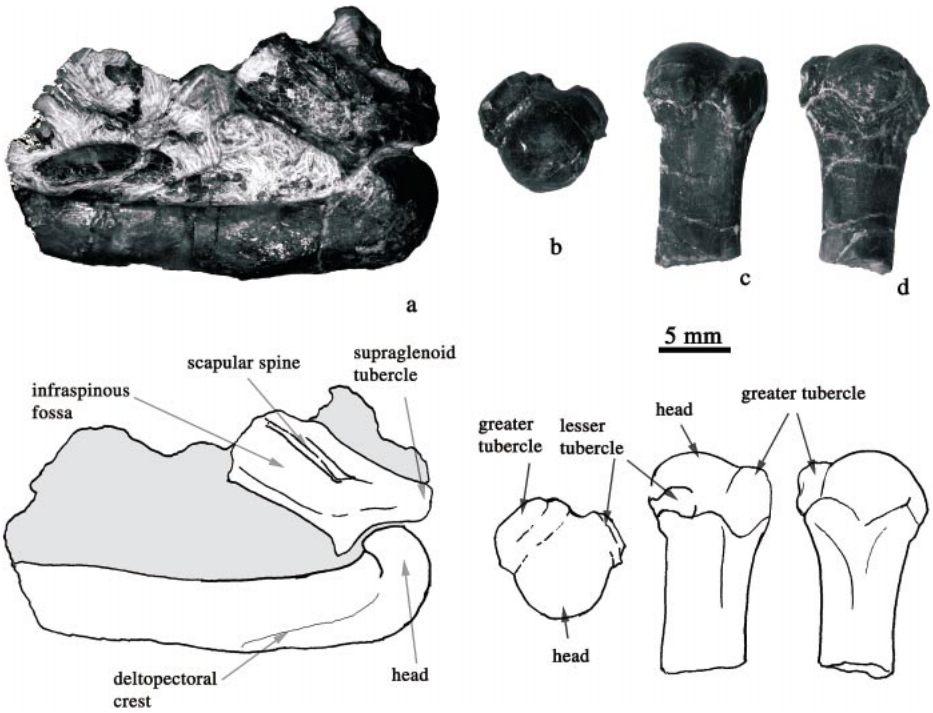

Fig. 14. **a,** Partial right scapula and humerus; **b–d,** proximal, ventral, and dorsal views of a proximal segment of the left humerus of *Matutinia nitidulus* (IVPP V7444).

The shape of this bone and its relationship to the surrounding elements suggest a composite nature: it probably represents the fused trapezoid and centrale. The magnum is narrow transversely and proximodistally elongate. It articulates with the third metacarpal distally. The unciform is the lateral element of the row. It contacts both the fourth and fifth metacarpals distally. Because of the narrow magnum, the unciform probably has a narrow contact with the third metacarpal as well.

The metacarpals are preserved, but the distal ends of the metacarpals I–IV are broken. Metacarpal I is very short and robust. It is largely located on the medial side of the trapezium. The ventral side of the bone bears a rounded fossa. The first phalanx is about 1.5 times as long as the first metacarpal. On the plantar surface, the distal end of the phalanx is narrower than the proximal; the lateral and medial condyles are equal in size. The first ungual phalanx is preserved, but its tip is broken. It is transversely narrow and has a well-developed plantar tubercle. The lengths of the metacarpals II–IV cannot be determined because of the broken distal ends. The diameters of metacarpals II and III are roughly equal and are reduced laterally from the metacarpal IV to V. Metacarpal V is the slimmest of the five; it is about the total length of the metacarpal I and phalanx I. Several sesamoid bones are preserved on the plantar side of the manus.

Some vertebrae in articulation are preserved with the pelvic girdle (fig. 16). The posterior part of the presumed sixth and the entire seventh lumbar vertebrae are preserved. The transverse process is narrow and projects anterolaterally. The spinous process is broken. The centrum of the last lumbar is rectangular, anteroposteriorly elongate, and has a very weak ventral keel. Three sacral vertebrae are preserved, and they are not fused. In ventral or dorsal view, the width of the vertebral body decreases from the lumbar to the third sacral vertebra. The morphology of the sacral vertebra is similar to that of the lumbar, except that the transverse process expands to a broad, flat wing, which distin-

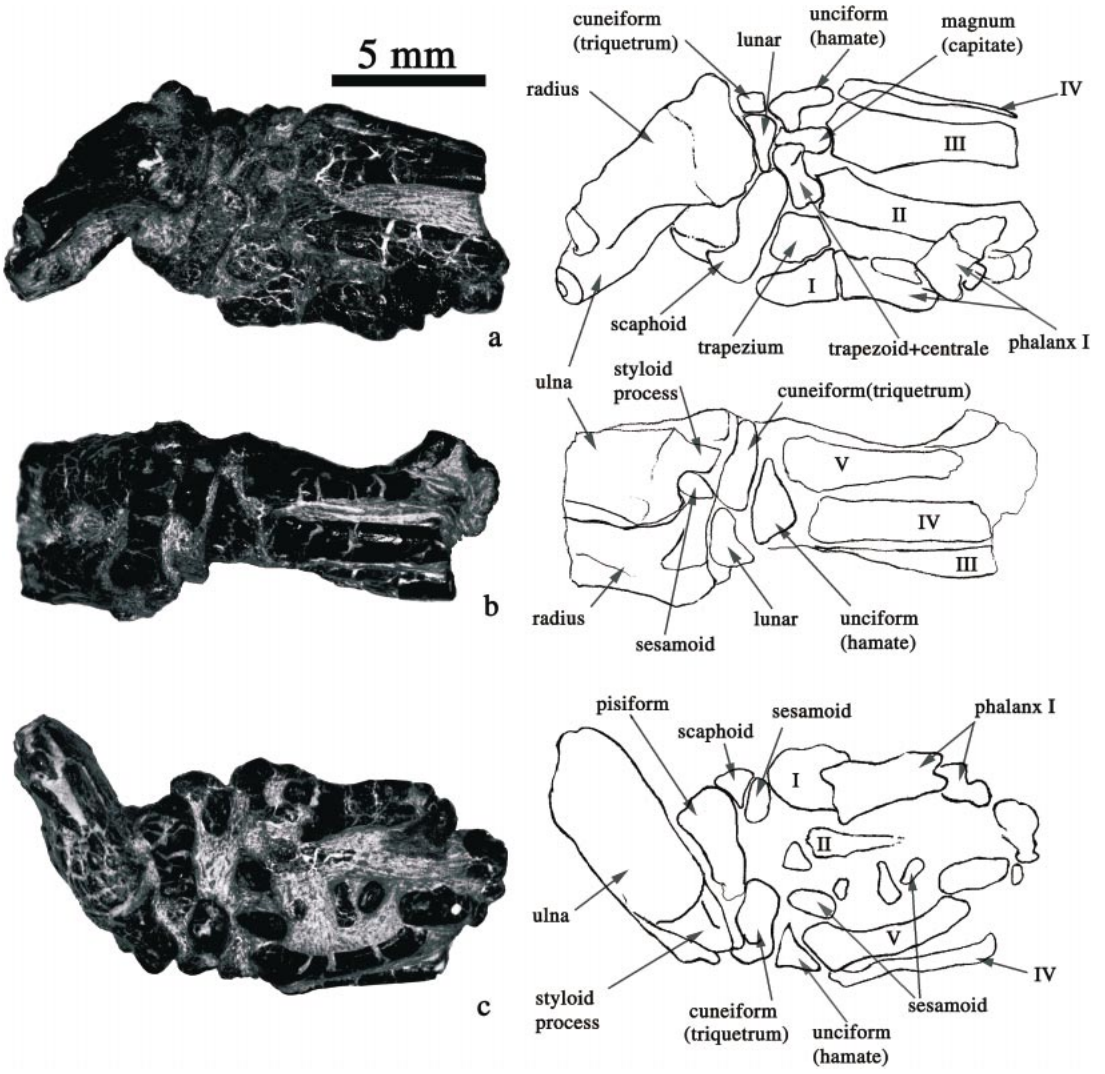

Fig. 15. Dorsal, lateral, and ventral (plantar) views of the left manus of *Matutinia nitidulus* (IVPP V7444).

guishes them from the caudal vertebrates. The wing of the first sacral vertebra is the widest, and it articulates with the pelvic girdle at the sacropelvic surface on the ilium. Only the anterolateral tip of the second sacral wing contacts the ilium.

The pelvic girdle is nearly complete, although the pubis, the acetabulum, and the symphysis of the pelvis cannot be seen clearly because of poor preservation (fig. 16). The ilium is slender and rodlike, without a flared wing. The anterior end of the ilium is broken. In dorsal and ventral views, the ilium is directed primarily anteriorly and slightly laterally. The gluteal surface is narrow. The dorsal and ventral borders of the ilium are thinner than the body. The posterodorsal iliac spine is distinct and is followed posteriorly by a deep greater ischiatic notch. Ventral to the notch, the iliopubic eminence is prominent. The head of the right femur is articulated in situ with the right acetabular fossa. Because of poor preservation, the shape of the acetabular fossa cannot be determined. The ischium is complete on both sides of the pelvic girdle. It is a transversely thin bone

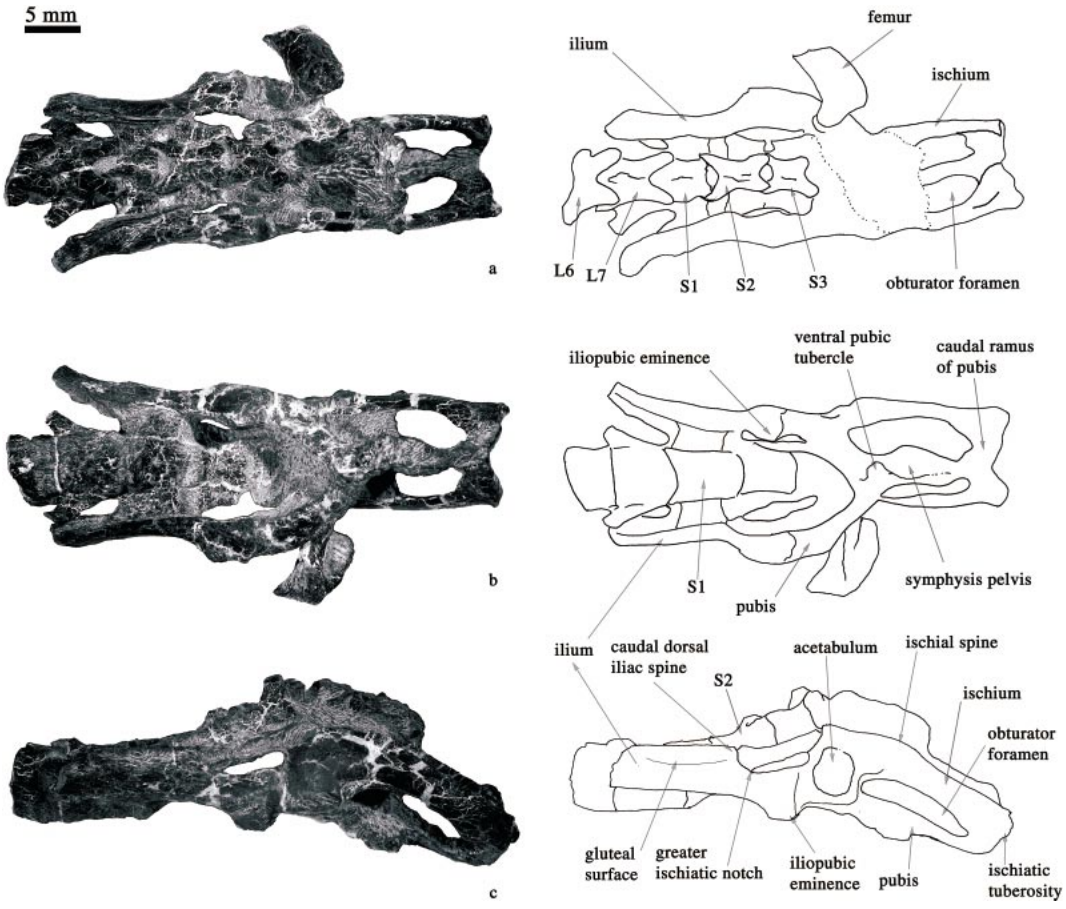

Fig. 16. Dorsal, ventral, and lateral views of the pelvic girdle of *Matutinia nitidulus* (IVPP V7444).

with a convex dorsal edge, of which the greatest curvature is at the weak ischial spine. The ventral edge of the ischium is dorsally concave, forming the dorsal border of a kidney-shaped obdurator foramen. The ischiatic tuberosity is a thickened plate with a rugged posterior surface. In this region, the dorsal edge and the posterior border of the ischium define a right angle. The maximum space between the ischia is 6 mm, but some distortion of the pelvic girdle during preservation may have altered the distance. The medial surface of the ischium is gently concave. Sutures between bones are unclear. By position, the pubic bone on each side of the girdle starts from the ventral side of the acetabular fossa, extends posteromedially, and merges at the pubic tubercle.

Only the left femur and partial proximal end of right femur are preserved (figs. 16, 17). They are articulated with the pelvis. The left femur also articulates with the tibia and fibula. The hindlimb was removed from the pelvis during preparation. The head of the left femur is broken. From the tip of the greater trochanter to the distal end, the femur is 18 mm long, which is shorter than the tibia (21 mm, not including the distal epiphysis of the tibia, which was detached but is preserved in articulation with the pes). The head of the femur is not well preserved on either side. The femoral neck is short. The greater trochanter is robust and is as proximally extended as the head; it projects ventrally as a ridge that bounds the deep trochanteric fossa laterally. The lesser trochanter is robust, projecting ventromedially. The narrowest region of the femur is distal to the lesser trochanter.

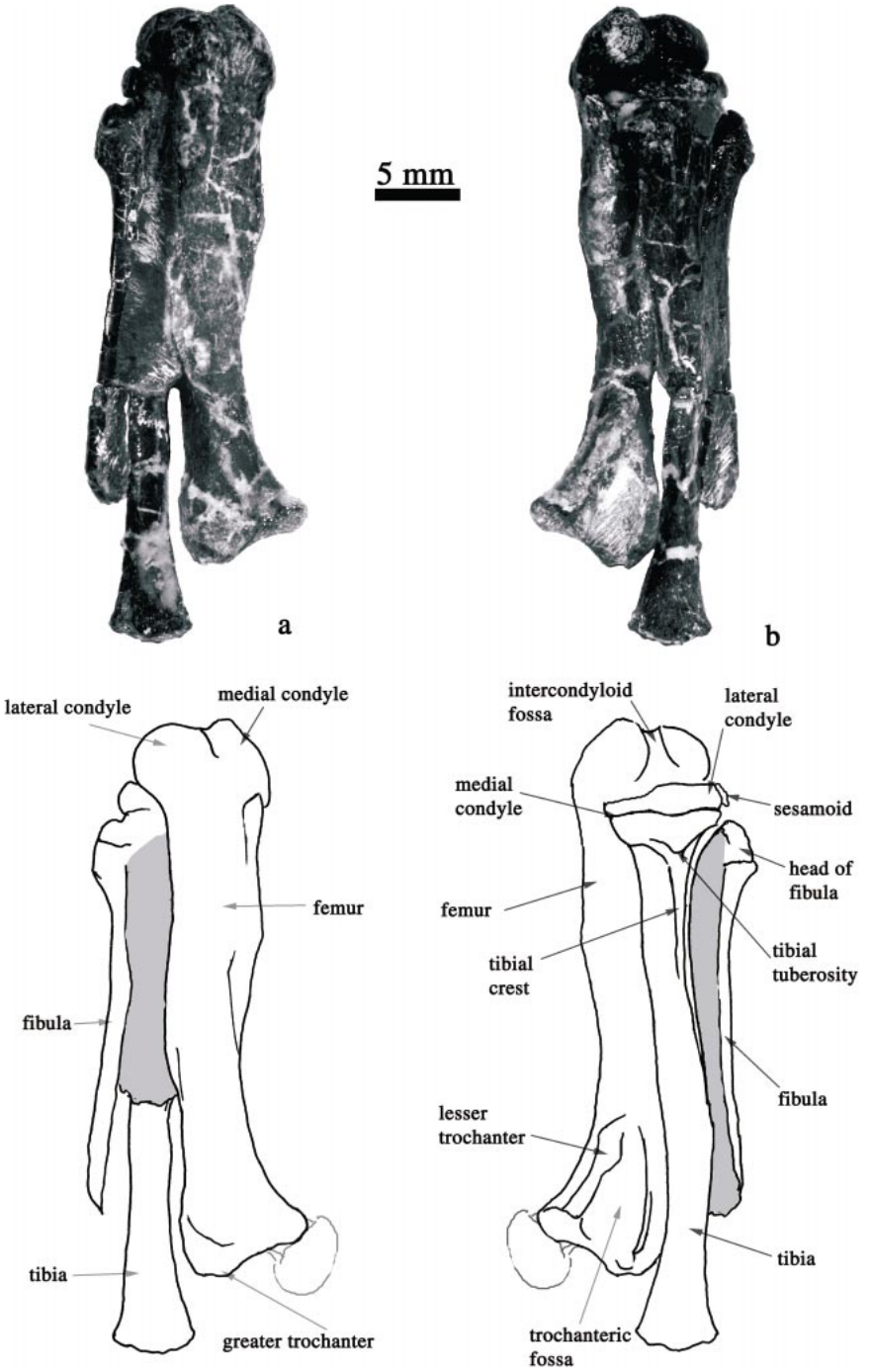

Fig. 17. Dorsal and ventral (for femur) views of the left femur, tibia, and fibula of *Matutinia nitidulus* (IVPP V7444).

The distal shaft of the femur is wide and dorsoventrally compressed. The compression may partly owe to postmortem crushing; otherwise, the shaft is unusually flat. Presence or absence of the third trochanter is unclear because of breakage. Also because of breakage, the shape of the patellar trochlea cannot be certain, but it appears to be shallow and narrow. The lateral condyle is slightly larger than the medial condyle. The intercondyloid fossa is deep and well defined. The lateral surface of the medial condyle is more concave than the medial surface of the lateral condyle.

The tibia is robust proximally and slender distally. The medial and lateral condyles are both blunt, on the proximal ends of which the articular facets to the condyles of the femur are concave and shallow, separated by a low intercondyloid eminence. A sesamoid bone is present at the lateral condyle of the tibia. The tibial tuberosity is relatively large and triangular. The tibial crest is strong and extends dorsally along one-third of the body of the tibia. The distal epiphysis of the tibia is detached from the shaft and is preserved in association with the astragalus in the pes. The posterior process of the tibia is distinct. The proximal portion of the left fibula is preserved. The fibula is slender and is completely separated from the tibia. The head is expanded and irregular in shape; it does not articulate with the femur, but only contacts the lateral condyle of the tibia.

All left tarsal bones, except for the calcaneus, are preserved in articulation (fig. 18). The distal epiphysis of the tibia is associated with the dorsal side of the astragalus, but it has been displaced, so that the tibial posterior process contacts the medial side of the astragalus. The astragalus is flat dorsal-plantarly, having a short, narrow neck and a large, transversely extended head. The trochlea of the astragalus is asymmetrical, with the lateral crest being larger than the medial. The lateral process is distinct. The groove of the trochlea is broad on the dorsal side but indistinct on the ventral side. At the lateral side, the articular surface for the fibula, the astragalofibular facet, is broad and slightly concave. Ventral to the astragalofibular facet is the calcaneoastragalar facet; the latter is narrower than the former. The distal parts of the two facets confine a right angle, whereas the angle increases proximally. The medial astragalotibial facet (not visible in fig. 18) is large and concave. The sulcus astragali and sustentacular hinge are broad and deep. Distal to the sulcus is the sustantacular facet, which is large, oval, and gently convex. In ventral view, the astragalonavicular facet is wider medially than laterally, whereas in distal view, the lateral facet is broader than the medial.

The navicular is large and irregular; its concave distal articular surface braces the head of the astragalus. The body is short proximodistally and extends transversely. The articular facet with the cuboid is concave. The plantar process is long, tongue-shaped, and dorsoventrally flat. It extends anteriorly to underlie the entire mesocuneiform. Medially, the navicular contacts primarily with the entocuneiform. A small sesamoid bone that articulates with both the navicular and the entocuneiform is considered the medial tarsal. The cuboid lateral to the navicular is blocky, being wider than long. Unlike the navicular, the proximal surface of the cuboid, which articulates with the calcaneus, is flat. In dorsal view, the cuboid has a narrow contact with the navicular and a broader one with the ectocuneiform. The articular facet of the ectocuneiform forms a deep fossa. In ventral view, the cuboid is wider than long. The surface is transversely convex and proximodistally concave. The plantar tubercle is a liplike projection and is transversely elongated. The plantar process floor has a broad, transversely long peroneal groove. Within the groove, there seems to be a small foramen filled with matrix. The distal end of the cuboid articulates with metatarsals IV and V.

The entocuneiform is proximodistally long, being wider distally than proximally. It articulates with the navicular laterally, but not with the astragalus owing to the medial tarsal that is situated between the astragalus and the entocuneiform. The identification of the medial tarsal is not certain because of its small size (see below). The broader distal end of the entocuneiform articulates with metatarsal I with a concave articular facet. The mesocuneiform is the smallest bone of the tarsus and is rectangular in dorsal view. Its plantar side is completely dorsal to the

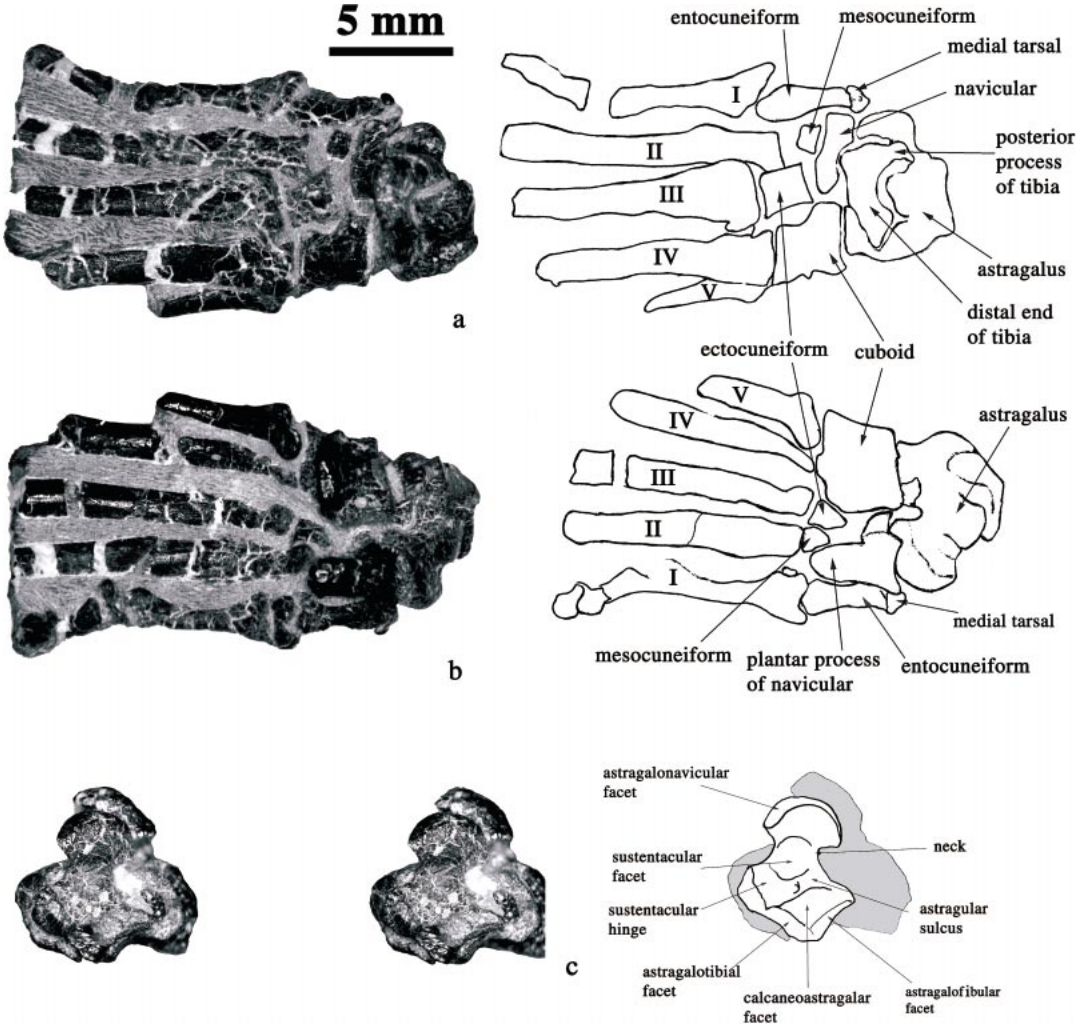

Fig. 18. **a, b,** Dorsal and ventral (plantar) views of the left pes of *Matutinia nitidulus* (IVPP V7444); **c,** dorsal view of the left astragalus.

plantar process of the navicular and therefore is not visible in ventral view. Proximally, the mesocuneiform contacts the medial side of the navicular and, distally, metatarsal II. The ectocuneiform is square-shaped in dorsal view. Its plantar process is robust. Its proximal end articulates with the navicular medially and with the cuboid laterally; its distal end, with metatarsal III.

Only the first digit is completely preserved. Metatarsal I has a robust proximal head, which extends proximomedially to the side of the entocuneiform. The first phalanx is about half the length of metatarsal I. The first ungual phalanx is similar to that of the manus in being transversely narrow and has a well-developed plantar tubercle, but it is shorter than that of the manus. The lengths of metatarsals II–V are unknown because of broken distal ends in all. Metatarsals II–IV are of similar width, whereas metatarsal V is the slenderest digit. The proximal end of metatarsal II is more proximally positioned than in other metatarsals.

DISCUSSION

Matutinia was originally compared to *Heomys* and *Rhombomylus* (Li et al., 1979).

Rhombomylus is represented by excellent skull and skeletal material, in contrast to fragmentary specimens of *Heomys* (Li, 1977; Ting and Li, 1984; Li and Ting, 1985, 1993), so that comparisons are limited. Regarding the dentition, *Matutinia* is unquestionably more similar to *Rhombomylus* than to *Heomys* in sharing the following features. Most distinctive is the expanded hypocone shelf on the upper cheek teeth, both molars and premolars. Although the hypocone and postcingulum are also prominent in other eurymylids, such as *Eurymylus* and *Heomys* (Matthew and Granger, 1925; Matthew et al., 1929; Sych, 1971; Li, 1977; Li and Ting, 1985), the postcingulum is not expanded to form a broad shelf. The complex zygoma in both *Rhombomylus* and *Matutinia* appears to be unique in having several processes from the jugal and maxilla. However, the zygoma is not preserved in other eurymylids, making comparisons impossible. The only exceptions are the specimens of *Eurymylus* described by Sych (1971), which display a different pattern of zygomatic process (see below). The basicranial regions in *Rhombomylus* and *Matutinia* similarly have a well-developed bulla that completely covers the middle tympanic cavity. Also present in both is an inflated mastoid of the petrosal that forms a bulbous shell posterior to the bulla and is exposed on the skull roof. The external auditory meatus in both is transversely long and functions also as the postglenoid process. A large postglenoid foramen is located at the posteromedial corner of the glenoid fossa in both genera. *Rhombomylus* and *Matutinia* are also similar in morphology of the astragalus, which is dorsoventrally flat and has a transversely extended head and astragalonavicular facet.

Matutinia differs from *Rhombomylus* in the following aspects. *Matutinia* is smaller. Its teeth are generally more primitive than those of *Rhombomylus*, having relatively lower crowns but more distinctive cusps and ridges. The p3 is single-rooted in *Matutinia* but double-rooted in *Rhombomylus*. On the upper teeth of *Rhombomylus*, the vertical groove on the lingual side of the cheek teeth extends into the alveolus, whereas the groove is partial in *Matutinia*. The paracone and metacone of *Matutinia* are more conical than those of *Rhombomylus*. These cusps and the protoloph and metaloph are also more distantly separated in *Matutinia* than in *Rhombomylus*. The hypocone shelf of the cheek teeth is more prominent in *Rhombomylus* than in *Matutinia*. In particular, the shelf on M3 of *Rhombomylus* forms a lobe with complex surface structures on unworn specimens. The hypocone shelf on M3 of *Matutinia* is simple and reduced. The ridges that confine the trigonid, the cristid obliqua (ectolophid), and talonid cusps are all recognizable in *Matutinia*, but not in *Rhombomylus*, even in very young individuals. *Matutinia* further differs from *Rhombomylus* in retaining the carotid foramen in the basicranial region. Although there is a foramen for the stapedial artery on the posteromedial side of the bulla in *Rhombomylus*, that foramen appears further reduced and apparently cannot contain a functional artery. The promontorium is more inflated with two apparent bulges, and the internal auditory meatus is much deeper in *Rhombomylus* than in *Matutinia*; the mastoid of the petrosal in the former is also more expanded than in the latter. The dorsal exposure of the mastoid process of *Matutinia* is smaller, and bony septa in the mastoid process of *Matutinia* are less well developed than those of *Rhombomylus*.

Heomys differs from *Matutinia* and *Rhombomylus* in being smaller and having more cuspate, lower-crowned cheek teeth with a less well-developed hypocone shelf. The P3 is double-rooted in *Heomys*, but has three roots in the other two genera. However, the P3 of *Heomys* is bicuspid, having a distinctive paracone labially and protocone lingually, with very weak crests connecting them anteriorly. Based on remaining roots in the alveolus (Li and Ting, 1985), the p3 of *Heomys* is double-rooted, as in *Rhombomylus*. In *Heomys*, the M1 is distinctly larger than the other cheek teeth. The incisive foramina in *Heomys* are larger and more posteriorly located than in *Rhombomylus*.

Eurymylus differs from *Matutinia* and *Rhombomylus* in having a less expanded hypocone shelf. The crowns of *Eurymylus* check teeth are generally lower than in *Matutinia* and *Rhombomylus*. The lower molars are more lagomorphlike. The trigonid on m1 and m2 is as wide as the talonid, and the

talonid is anteroposteriorly shortened, in contrast to a relatively longer talonid in *Matutinia* and *Rhombomylus*. As shown in the specimens described by Sych (1971: MgM-II/62–64), best displayed in MgM-II/64, a bony ridge extends posterolaterally on the ventral side of the anterior process of the zygomatic arch. Dorsal to the ridge, on the anterior process of the lateral surface of the arch, there is a distinct fossa. The zygoma of MgM-II/64 was not originally illustrated by Sych, but it is clear from a stereophotograph that we have examined. The dentition of MgM-II/64, however, more closely resembles that of *Matutinia* than other specimens referred to *Eurymylus* by Sych. This suggests that MgM-II/64 may represent a different species, as noted by McKenna and Meng (2001). MgM-II/64 is closely comparable to a specimen described by Dashzeveg and Russell (1988: fig. 5; PSS 20–162). In addition, *Eurymylus* has much longer incisive foramina, ending posteriorly at the level of P3. The rostrum of *Eurymylus* is abruptly narrowed anterior to the infraorbital foramen, whereas it tapers gradually anteriorly in *Matutinia* and *Rhombomylus*.

Other eurymylids, including *Niklomylus* (Shevyreva and Gabunia, 1986), *Zagmys* (Dashzeveg et al., 1987), *Asiaparamys* and *Kazygurita* (Nessov, 1987), *Eomylus*, *Amar*, and *Khaychina* (Dashzeveg and Russell, 1988), *Aktashmys* (Averianov, 1994), and *Decipomys* (Dashzeveg et al., 1998), can be easily differentiated from *Matutinia* and *Rhombomylus* by the dental and other features listed above for the two genera.

A review of the internal carotid system in rodents indicates that its presence is a primitive feature within eutherians, whereas its loss is derived and probably occurred more than once (Meng, 1990). However, the position in relation to the auditory region and branching pattern of the internal carotid system are not fully understood within early glireid mammals. It is now generally accepted that a coeval internal carotid artery and stapedial artery on the ventral surface of the promontorium, which may or may not leave impressions on the bone, is the primitive eutherian condition (MacPhee, 1981; Wible, 1983, 1986, 1987). This condition is observed in sciuravids (Wahlert, 1974; Meng, 1990), theridomorphs (Lavocat and Parent, 1985), and *Cocomys* (Li et al., 1989). Some paramyines are said to have this pattern (Lavocat and Parent, 1985), but the condition has not been clearly observed in *Paramys* (Meng, 1990). At least three derived conditions of the internal carotid system exist in rodents. First, the promontory branch is lost, while the stapedial artery is still present, as in *Reithroparamys* (Meng, 1990). Second, both arteries are present, but their bifurcation is medial to the medial bullar wall, as in *Rattus* (Wible, 1987). Finally, the entire internal carotid system is lost, as in *Tsaganomys* (Bryant and McKenna, 1995). In this regard, *Matutinia* presents an interesting case that appears to be similar to the condition of *Rattus*. An extratympanic bifurcation of the internal carotid and stapedial arteries in *Rhombomylus* was implied by Ting and Li (1984), although the identification of the foramen for the internal carotid artery in *Rhombomylus* was questioned (Meng, 1990). With observations of more and better preserved skulls of *Rhombomylus*, it is clear that the carotid foramen is absent in this genus. In *Matutinia*, however, the coexistence of three foramina, interpreted as jugular, carotid, and stapedial, is unquestionable and is convincing evidence for an extratympanic bifurcation of the internal carotid artery. The *Rhombomylus* condition is more derived than that of *Matutinia* by loss of the internal carotid artery and the foramen transmitting it. Moreover, the foramen for the stapedial artery in *Rhombomylus* is further reduced than in *Matutinia* and probably is not functional. Meng (1990) speculated that if the *Rhombomylus* condition as interpreted by Ting and Li (1984) proves to be true, the extratympanic bifurcation may serve as evidence for an eurymylid-rodent relationship. However, given the primitive condition in *Cocomys* and sciuravids, it is more prudent to interpret the condition in *Matutinia* as an independent evolution rather than as a synapomorphy between eurymylids and rodents.

The manus of *Matutinia* is the only known specimen of this region in eurymylids. In general, it has some primitive features in comparison with that of rodents. It has five digits. The scaphoid and lunar are unfused, a condition considered a feature characteris-

tic of the family Paramyidae (Matthew, 1910). However, in the study of the manus of *Douglassia jeffersoni* (= *Protosciurus jeffersoni*; see Emry and Korth, 1996 for taxonomic note), Emry and Thorington (1982) showed that this condition is variable in paramyids. According to Emry and Thorington (1982), unfused scaphoid and lunar is a primitive condition in rodents; therefore, it cannot be used to diagnose the family Paramyidae, nor does it indicate any special relationship to *Douglassia*, which retains the primitive condition. Given the outgroup relationships of eurymylids to Rodentia (Meng et al., 1994; Meng and Wyss, 2001), presence of unfused scaphoid and lunar in *Matutinia* supports Emry and Thorington's conclusion. In fact, this is undoubtedly the primitive condition for eutherian mammals, because it is present in *Asioryctes* (Kielan-Jaworowska, 1977), marsupials (Szalay, 1994), and symmetrodonts (Hu et al., 1997, 1998).

Although a fused scapholunar is characteristic of almost all living rodents, the five elements in the distal row of the carpus are commonly separated, as shown in *Rattus*, *Myocastor*, and *Marmota*. The presence of five elements is probably primitive in mammals, because they occur in *Asioryctes* (Kielan-Jaworowska, 1977) and symmetrodonts (Hu et al., 1997, 1998). In marsupials, however, the centrale is commonly absent (Szalay, 1994). There are four elements in the distal row of the carpus of *Matutinia*. We interpret that the trapezoid and centrale of *Matutinia* are fused. This is based on the observation that the medial part of the fused bone is in contact with the third metacarpal and the lateral part with the lunar and scaphoid. This relationship reflects that in the primitive condition, the centrale is in contact with the lunar and scaphoid proximally and the trapezoid with metacarpal II distally. We are not aware of fusion of the trapezoid and centrale in other mammals, and we tentatively consider this condition as an autapomorphy for *Matutinia*.

Matutinia is similar to rodents in that the distal (ungual) phalanges are dorsoventrally deep and laterally compressed, and that the thumb is short, with the metacarpal being medial to the trapezium. Emry and Thorington (1982) recognized that a reduced first digit is a characteristic of the order Rodentia. The manus of *Matutinia* shows that the thumb of eurymylids is shortened, which is probably a derived condition in eutherians, because the first digit is relatively long in *Asioryctes* (Kielan-Jaworowska, 1977). However, a shortened thumb in other mammals, such as carnivores, indicates independent acquisition of the feature within several eutherian lineages. In carnivores, the first metacarpal has an end-to-end articulation with the trapezium, which is the primitive condition because it is present in *Asioryctes* (Kielan-Jaworowska, 1977), marsupials (Szalay, 1994), and symmetrodonts (Hu et al., 1998). In contrast, the side-to-side contact in *Matutinia* and rodents is probably derived.

In comparison with many rodents, such as *Douglassia* (Emry and Thorington, 1982) and *Paramys* (Wood, 1962), the sacrum of *Matutinia* is primitive in that the sacral vertebrae are not fused, and the wing of the second sacral vertebra has limited contact with the ilium. The sacroiliac joint is made by articulation of the first and second sacral vertebrae with the ilium in rodents, and by only the first sacral vertebra in extant lagomorphs. Bones of the pelvic girdle are all slim, showing no expansion in any direction. The lesser trochanter of the femur projects more ventrally in *Matutinia*, but it is more medially directed in *Douglassia* (Emry and Thorington, 1982) and *Paramys* (Wood, 1962; personal. obs.). The third trochanter is more distally located in paramyids than in living rodents (Emry and Thorington, 1982). The shape of the third trochanter cannot be surely determined in *Matutinia* because of breakage, but it is probably less distally positioned than that of *Paramys*. The fibula is primitively unfused to the tibia in *Matutinia*, but it is proportionally slimmer than that of *Paramys*, similar to the condition of some living rodents, such as *Sciurus* and *Rattus*. In addition, the fibula and tibia are less arched than those of living rodents. Szalay (1985) noted a distinct posterior process of the tibia in paramyids and other rodents in which the element is known, and he considered it evidence for lepticitid–rodent relationships. The posterior process of the tibia in *Matutinia* is prominent, similar to that of rodents.

The tarsus figures heavily in phylogenetic reconstruction of the Glires (Bleefeld and McKenna, 1985; Szalay, 1985; Averianov, 1994; Meng and Wyss, 2001). The astragalus of *Matutinia* is generally more similar, probably primitively, to those of *Tribosphenomys* (Meng and Wyss, 2001) and *Paramys* (Wood, 1962) in being dorsoventrally flat and in having a transverse head and astragalonavicular facet. However, the astragular head in *Paramys* is more medially extended, and the astragular neck of *Tribosphenomys* is wider than in *Matutinia*. In *Tribosphenomys* and *Matutinia*, the crests of the trochlea are less sharp than those of rodents and lagomorphs. The astragalus of *Matutinia* differs from those of lagomorphs and their relatives (Bohlin, 1951; Dawson, 1958; Bleefeld and McKenna, 1985; Szalay, 1985; Averianov, 1994). In those forms the astragalus is laterally compressed, in which there are sharp delineations between articular surfaces, and the navicular facet of the astragalus extends onto the dorsal surface of the neck.

Szalay (1985) has discussed the nature of the medial tarsal, a sesamoid bone present only in rodents. He noted that arboreal squirrels seem to have a relatively larger medial tarsal than do various terrestrial murids, probably related to arboreal climbing that applies a greater force to the foot. Szalay (1985) considered that whether this bone was present in more primitive eutherians predating the first rodent could not be determined based on available fossils. The pes of *Matutinia* shows that the medial tarsal did exist in rodent relatives, and its small size is suggestive of a terrestrial species, following Szalay (1985).

In summary, based on more complete material, we have provided additional morphological differences between the *Matutinia* and *Rhombomylus* and between them and other eurymylids. These additional distinctive features in *M. nitidulus* contradict the statements that no diagnostic distinguishing features of generic value are evident from the lower teeth and that a difference in shape of the M3 appears to be the major distinction separating *M. nitidulus* from *R. turpanensis* (Dashzeveg and Russell, 1988). Therefore, the basis for considering *Matutinia* as a junior synonym of *Rhombomylus* no longer exists. Nonetheless, whether the two taxa should be treated as two species of the same genus or as different genera is is still subjective decision, no matter how many differences may have existed. Based on the features recognized in this study, we presently prefer to consider *Matutinia* and *Rhombomylus* as two closely related genera, and therefore resurrect the monotypic genus *Matutinia* for *M. nitidulus*.

ACKNOWLEDGMENTS

This paper is derived from Ting's dissertation. Ting gratefully recognizes the members of her Ph.D. committee—J.A. Schiebout, M.S. Hafner, J.E. Hazel, J.M. Lorenzo, B.K. Sen Gupta, and R.G. Tague from Louisiana State University (LSU), and M.C. McKenna from the American Museum of Natural History and Columbia University—who gave their advice and support throughout the course of her research. Ting's special thanks go to J.-l. Li and S.-h. Xie of the Institute of Vertebrate Paleontology and Paleoanthropology, Chinese Academy of Sciences, Beijing, for their assistance during the field trip to the Hengyang Basin in 1987, and to J.A. Schiebout for her support in this research. M.L. Eggart of LSU drew the map in figure 1. R.B. Hubert of LSU helped improve the English of the manuscript. R.C. Hulbert, Jr., Z.-x. Luo, and two anonymous reviewers made useful comments that significantly improved the study. Meng's research has been supported by an NSF grant (DEB-9796038), special funds for major state basic research projects of China (G200007707), and an NSFC grant (no. 49928202).

REFERENCES

Averianov, A.O. 1994. Early Eocene mimotonids of Kyrgyzstan and the problem of Mixodontia. Acta Palaeontologica Polonica 4: 393–411.

Bleefeld, A.R., and M.C. McKenna. 1985. Skeletal integrity of *Mimolagus rodens* (Lagomorpha, Mammalia). American Museum Novitates 2806: 1–5.

Bohlin, B. 1951. Some mammalian remains from Shi-her-ma-cheng, Hui-hui-pu area, Western Kansu. Report from the scientific expedition to the Northwestern provinces of China under leadership of Dr. Sven Hedin, Publication 35, Vertebrate Palaeontology 5: 1–47.

Bryant, J.D., and M.C. McKenna. 1995. Cranial anatomy and phylogenetic position of *Tsaganomys altaicus* (Mammalia: Rodentia) from the Hsanda Gol Formation (Oligocene), Mongolia. American Museum Novitates 3156: 1–42.

Dashzeveg, D., J.-L. Hartenberger, Martin, T., and S. Legendre. 1998. A peculiar minute Glires (Mammalia) from the early Eocene of Mongolia. Bulletin of the Carnegie Museum of Natural History 34: 194–209.

Dashzeveg, D., and D.E. Russell. 1988. Palaeocene and Eocene Mixodontia (Mammalia, Glires) of Mongolia and China. Palaeontology 31: 129–164.

Dashzeveg, D., D.E. Russell, and L.J. Flynn. 1987. New Glires (Mammalia) from the early Eocene of the People's Republic of Mongolia. 1. Systematics and description. Proceedings of the Koninklijke Nederlandse Akademie Van Wetenschappen B 90: 133–154.

Dawson, M.R. 1958. Later Tertiary Leporidae of North America. University of Kansas Paleontological Contributions, Vertebrata, Article 6: 1–75.

Emry, R.J., and W.W. Korth. 1996. The Chadronian squirrel *''Sciurus'' jeffersoni* Douglass, 1901: A new generic name, new material, and its bearing on the early evolution of Sciuridae (Rodentia). Journal of Vertebrate Paleontology 16: 775–780.

Emry, R.J., and R.W. Thorington. 1982. Descriptive and comparative osteology of the oldest fossil squirrel, *Protosciurus* (Rodentia: Sciuridae). Smithsonian Contributions to Paleobiology 47: 1–35.

Hu, Y.-m., Y.-q. Wang, Z.-x. Luo, and C.-k. Li. 1997. A new symmetrodont mammal from China and its implications for mammalian evolution. Nature 390: 137–142.

Hu, Y.-m., Y.-q. Wang, C.-k. Li, and Z.-x. Luo. 1998. Morphology of dentition and forelimb of *Zhangheotherium*. Vertebrata PalAsiatica 36: 102–125.

Kielan-Jaworowska, Z., 1977. Evolution of the therian mammals in the Late Cretaceous of Asia. Part II. Postcranial skeleton in *Kennalestes* and *Asioryctes*. Palaeontologia Polonica 37: 65–83.

Lavocat, R., and J.-P. Parent. 1985. Phylogenetic analysis of middle ear features in fossil and living rodents. *In* W.P. Luckett, and J.-L. Hartenberger (editors), Evolutionary relationships among rodents—a multidisciplinary analysis: 333–354. New York: Plenum.

Li, C.-K. 1977. Paleocene eurymyloids (Anagalida, Mammalia) of Qianshan, Anhui. Vertebrata PalAsiatica 15: 103–118.

Li, C.-K., C.-s. Chiu, D.-K. Yan, and S.-H. Hsieh. 1979. Notes on some early Eocene mammalian fossils of Hengdung, Hunan. Vertebrata PalAsiatica 17: 71–80.

Li, C.-K., and S.-Y. Ting. 1985. Possible phylogenetic relationships of eurymylids and rodents, with comments on mimotonids. *In* W.P. Luckett, and J.-L. Hartenberger (editors), Evolutionary relationships among rodents: 35–58. New York: Plenum.

Li, C.-K., and S.-Y. Ting. 1993. New cranial and postcranial evidence for the affinities of the eurymylids (Rodentia) and mimotonids (Lagomorpha). *In* F.S. Szalay, M.J. Novacek, and M.C. McKenna (editors), Mammal phylogeny-placentals: 151–158. New York: Springer-Verlag.

Li, C.-K., R.W. Wilson, M.R. Dawson, and L. Krishtalka. 1987. The origin of rodents and lagomorphs. *In* H.H. Genoways (editor), Current Mammalogy 1: 97–108. New York: Plenum.

Li, C.-K., J.-J. Zheng, and S.-Y. Ting. 1989. The skull of *Cocomys lingchaensis*, an Early Eocene Ctenodactyloid Rodent of Asia. *In* C.C. Black and M. Dawson (editors), Papers on fossil rodents in honour of Albert Elmer Wood. Natural History Museum, Los Angeles County, Science Series 33: 179–192.

MacPhee, R.D.E. 1981. Auditory regions of primates and eutherian insectivores. Morphology, ontogeny, and character analysis. Contributions to Primatology 18: 1–282.

Matthew, W.D. 1910. On the osteology and relationships of *Paramys* and the affinities of the Ischyromyidae. Bulletin of the American Museum of Natural History 28: 43–72.

Matthew, W.D., and W. Granger. 1925. Fauna and correlation of the Gashato Formation of Mongolia. American Museum Novitates 189: 1–12.

Matthew, W.D., W. Granger, and G.G. Simpson. 1929. Additions to the fauna of the Gashato Formation of Mongolia. American Museum Novitates 376: 1–12.

McKenna, M.C., and S.K. Bell. 1997. Classification of mammals above the species level. New York: Columbia University Press.

McKenna, M.C., and J. Meng. 2001. A primitive relative of rodents from the Chinese Paleocene. Journal of Vertebrate Paleontology 21: 565–572.

Meng, J. 1990. The auditory region of *Reithroparamys delicatissimus* (Rodentia, Mammalia) and its systematic implications. American Museum Novitates 2972: 1–35.

Meng, J., and A.R. Wyss. 1994. The enamel microstructure of *Tribosphenomys* (Mammalia, Glires): Functional and phylogenetic implica-

tions. Journal of Mammalian Evolution 2: 185–203.
Meng, J., and A.R. Wyss. 2001. The Morphology of *Tribosphenomys* (Rodentiaformes, Mammalia): phylogenetic implications for basal Glires. Journal of Mammalian Evolution 8: 1–71.
Meng, J., A.R. Wyss, M.R. Dawson, and R.-j. Zhai. 1994. Primitive fossil rodent from Inner Mongolia and its implications for mammalian phylogeny. Nature 370: 134–136.
Miller, M.E. 1964. Anatomy of the dog. London: W.B. Saunders, 941 pp.
Nessov, L.A. 1987. Results of search and investigation of Cretaceous and Early Paleogene mammals on the territory of the USSR. Ezhegodnik Vsesoyuznogo Paleontologicheskogo Obshchestva 30: 199–218. [in Russian]
Novacek, M.J. 1986. The skull of leptictid insectivorans and the higher-level classification of eutherian mammals. Bulletin of the American Museum of Natural History 183: 1–111.
Romer, A.S. 1966. Vertebrate Paleontology. Chicago: University of Chicago Press, 468 pp.
Shevyreva, N.S., and L. Gabunia. 1986. The first discovery of Eurymylidae (Mixodontia, Mammalia) in USSR. Journal of Palaeontology 4: 77–82. [in Russian]
Simpson, G.G. 1945. The principles of classification and a classification of mammals. Bulletin of the American Museum of Natural History 85: 1–350.
Sych, L. 1971. Mixodontia, a new order of mammals from the Paleocene of Mongolia. Palaeontologia Polonica 25: 147–158.
Szalay, F.S. 1985. Rodent and Lagomorph morphotype adaptations, origins, and relationships: some postcranial attributes analyzed. *In* W.P. Luckett, and J.-L. Hartenberger (editors), Evolutionary relationships among rodents—a multidisciplinary analysis: 83–132. New York: Plenum.
Szalay, F.S. 1994. Evolutionary history of the marsupials and an analysis of osteological characters. New York: Cambridge University Press.
Szalay, F.S., and M.C. McKenna. 1971. Beginnings of the age of mammals in Asia: the late Paleocene Gashato fauna, Mongolia. Bulletin of the American Museum of Natural History 144: 269–318.
Ting, S.-Y. 1995. An early Eocene mammalian fauna from Hengdong, Hunan Province, China. Ph.D. dissertation, Louisiana State University, Baton Rouge, 200 pp.
Ting, S.-Y., and C.-K. Li. 1984. The structure of the ear region of *Rhombomylus* (Anagalida, Mammalia). Vertebrate PalAsiatica 22: 92–102.
Wahlert, J.H. 1974. The cranial foramina of protrogomorphous rodents, an anatomical and phylogenetic study. Bulletin of the Museum of Comparative Zoology, Harvard University 146: 363–410.
Wible, J.R. 1983. The internal carotid artery in early eutherians. Acta Palaeontologica Polonica 28: 281–293.
Wible, J.R. 1986. Transformations in the extracranial course of the internal carotid artery in mammalian phylogeny. Journal of Vertebrate Paleontology 6: 313–325.
Wible, J.R. 1987. The eutherian stapedial artery: character analysis and implications for superordinal relationships. Zoological Journal of the Linnean Society, London 91: 107–135.
Wood, A.E. 1942. Notes on the Paleocene lagomorph, *Eurymylus*. American Museum Novitates 1162: 1–7.
Wood, A.E. 1962. The early Tertiary rodents of the family Paramyidae. Transactions of the American Philosophical Society of Philadelphia 52: 1–261.
Young, C.-C. 1944. Note on the first Eocene mammal from South China. American Museum Novitates 1268: 1–3.

Recent issues of the *Novitates* may be purchased from the Museum. Lists of back issues of the *Novitates* and *Bulletin* published during the last five years are available at World Wide Web site http://nimidi.amnh.org. Or address mail orders to: American Museum of Natural History Library, Central Park West at 79th St., New York, NY 10024. TEL: (212) 769-5545. FAX: (212) 769-5009. E-MAIL: scipubs@amnh.org